# A STUDY ON ENGINEERING BEHAVIOUR OF SCHIST ROCK

*A Thesis submitted in partial fulfilment of the requirements for the Degree of*

**Bachelor and Master of Technology (Dual Degree)**

in

**Civil Engineering**

*By*

**DHYANESHWAR MOTAMARRI**

*Under the guidance of*

**PROF. NAGENDRA ROY**

**DEPARTMENT OF CIVIL ENGINEERING**

**NATIONAL INSTITUTE OF TECHNOLOGY**

**ROURKELA-769008**

**MAY 2015**

DEPARTMENT OF CIVIL ENGINEERING

NATIONAL INSTITUTE OF TECHNOLOGY

ROURKELA – 769008, ODISHA, INDIA

---

# CERTIFICATE

This is to certify that the project entitled “A Study on Engineering Behaviour of Schist Rock” submitted by Mr. Dhyaneshwar Motamarri (Roll No. 710CE1152) in partial fulfilment of the requirements for the award of Bachelor and Master of Technology Dual Degree in Civil Engineering (Geotechnical Engineering) is an authentic work carried out by him under my supervision and guidance.

To the best of my knowledge, the matter embodied in this thesis has not been submitted to any other University/Institute for the award of any Degree or Diploma.

Date:

Place: Rourkela

Dr. Nagendra Roy
Professor
Department of Civil Engineering
National Institute of Technology
Rourkela - 769008

# ACKNOWLEDGEMENTS

I avail this wonderful opportunity to express my heartfelt gratitude to **Prof. Nagendra Roy** for his able guidance, support, encouragement, suggestions and the essential facilities provided to successfully complete the present research work. I truly appreciate and value his esteemed guidance and encouragement from beginning to the end of this thesis. His knowledge and company at the time of crisis will be remembered lifelong.

I am thankful to **Prof. Shishir Kumar Sahoo**, Head of the Department and all the faculty members of the Civil Engineering Department, especially the entire Geotechnical Engineering Specialization Group who have helped me throughout the project work.

I would also thank **Prof. Manoj Kumar Mishra** for granting me the permission to work in the Geomechanics Lab, Department of Mining Engineering and for providing the necessary help.

I would like to thank my parents for their blessings and wishes which has enabled me to complete the work successfully.

I bow to the Divine Power who led me all through.

Dhyaneshwar Motamarri

710ce1152

Geotechnical Engineering

Department of Civil Engineering

NIT Rourkela

# CONTENTS

# ABSTRACT

In the present world, many important rock structures are being planned, designed and constructed to meet the requirements of different civil and mining engineering applications. Knowing the various properties of the rock beforehand are requirement to assess the suitability of the rock for the particular application. Also, the strength of the rock is an important factor is effected to a significant extent due to the presence of joints and other defects in rock. Predicting the effect of joints on the strength of rock can help to large extent for making a better design of structure.

Keeping in view of the above, the present study has been carried out to find out the different physical and mechanical properties of schist rocks so as to understand the suitable applications based on the properties obtained. The effect of joints in Schist rock is studied, empirical relationships are proposed for predicting the strength of the rock for a given joint geometry. Also, numerical modelling is done to analyze circular tunnels of different diameters under different insitu stress ratios made by using the results as obtained from the different experiments which have been carried out.

# LIST OF FIGURES

# AND

# TABLES

# LIST OF FIGURES

# LIST OF TABLES

# NOMENCLATURE

| | | |
|---|---|---|
| PSI | : | Protodyakonov Strength Index |
| $J_f$ | : | Joint factor |
| $J_n$ | : | Number of joints per unit length |
| r | : | Roughness parameter |
| $\sigma_{cr}$ | : | Compressive strength ratio |
| $\sigma_{cj}$ | : | Compressive strength of the jointed rock specimen |
| $\sigma_{ci}$ | : | Compressive strength of the intact rock specimen |
| $E_{tr}$ | : | Elastic Modular ratio |
| $E_{tj}$ | : | Elastic Modulus of the jointed rock specimen |
| $E_{ti}$ | : | Elastic Modulus of the intact rock specimen |

# CHAPTER 1

# INTRODUCTION

# INTRODUCTION

## SCHIST ROCK

Schist rock is dominantly found in metamorphic regions such as Scotland, Norway or the Alps and in some parts of India. Schist rock is found mostly in Eastern and North-Eastern parts of India. The grain size in these rocks range from 0.1mm to 2 mm. Thus, these exist as medium grained and coarse grained rocks. These rocks form because of change in mineralogy and texture of existing rocks by heating and deep burial due to forces of plate tectonics. Thus, these rocks occur due to Regional Metamorphism. The existing rocks are mostly of igneous or sedimentary in nature. Schist has properties similar to that of slate as both are from similar rock types except that schist is subjected to more heat and temperature. The directional mineral nature of these rocks arises during crystallization under a stress. The properties of Schist rock not only depend on the nature of the parent rock but also on the pressure and temperature conditions. Greenschists and Blueschists have same parent rocks but are formed under different temperature and pressure conditions. Greenschists are formed due to high temperature and high pressure far below the earth whereas blueschists are formed under relatively low temperature and high pressure.

The structure of these rocks is mostly intact-foliated that is minerals in the rock mass have a preferred orientation of a planar nature. The common minerals present in these rocks are Mica, Chlorite, Talc, Graphite and Quartz. Depending on the prominent minerals present, the schist can be divided as Quartz Schist, Muscovite Schist, Mica Schist and so on. The minerals present in the rock may differ from those present in the parent rock before metamorphism. The silvery appearance of these rocks makes them suitable to be used for decorative purposes. Discontinuities in Schist rock is formed mostly by the schistosity planes which effect the engineering properties of rock such as its deformation and its strength. Depending on the minerals present which fulfils the presence of required property, the rock also finds its use in large number of applications such as road construction material, ballast for supporting railway sleepers, tunnel construction etc.

In the present study, detailed experimental investigation is carried on to study the different properties of Schist rocks and to its application based on the properties determined. Also, the behaviour of schist rocks is determined for different number of joints and at different joint orientations.

## TUNNELLING IN SCHIST ROCK

Underground tunnels satisfy the effective means for utilization of underground spaces. They also help in trying to control traffic congestion and environmental problems such as $CO_2$ emissions and optimization of energy usage. Also, underground structure in a crowded urban area imply changes on the natural habitat above the ground are very less. Apart from transportation purposes comprising of road vehicles, trains, subways etc. tunnels also serve for many other purposes such as conducting water and sewage, mining ores, underground hydroelectric-power plants and other military needs. Rock tunnels have an edge over the soil tunnels in providing more stability and less settlement.

Stability and settlement in tunnels are important factors whose estimation is very essential before a tunnel is made. This saves time, cost and effort to a large extent. Prediction of ground movement and analysis of tunnel stability and are made possible by the recent developments in the field of Finite Element Method. Plaxis is one such software which is based on Finite Element Method, using which estimation of behaviour of rock before drilling and finding out which part of the tunnel is under major settlement risk can be made.

An attempt has been made to study tunnels of different diameter under different insitu stress ratio with the properties of rock as obtained from the experimental results and thereafter analysed in terms of stress distribution and deformation using Plaxis software.

# CHAPTER 2

# LITERATURE REVIEW

# LITERATURE REVIEW

## Yaji et al. (1984)

They carried on triaxial and uniaxial compressive tests on different jointed rock models of Plaster of Paris, Sandstone and Granite. The investigation stated that (i) the friction angle remains almost same irrespective for the rock being jointed or intact (ii) the cohesion depends on the joint orientation, minimum at a joint orientation of 45º and as the roughness increases cohesion also increases (iii) The variation of uniaxial compressive strength of the rock is similar to that of cohesion and the ratio of uniaxial compressive strength to the cohesion value for a particular rock is almost constant (iv) The modulus parameters vary with orientation and roughness of the joint plane.

## Rao et al. (1984)

They carried on experimental investigation on four different types of Sandstones namely Kota, Singrauli, Jamrani and Jhingurda. The strength of these specimens at different relative humidity was tested. Triaxial test was carried on for different confining pressures. The strength of these specimens was also found out for different joint orientations. The results stated that the strength and modulus of elasticity decreases with increase in moisture content. Based on the results, a new empirical criterion is proposed between uniaxial compressive strength, deviator stress and confining stress.

## Srivastava et al. (1985)

They analysed the behaviour of single and deep interacting tunnels using elasto-plastic finite element method. Different aspects such as material behaviour, insitu stress ratio and spacing between the interacting tunnels were varied and analysis was done. Circular and horse-shoe tunnels of different sizes were considered for analysis. In case of interacting tunnels, the interaction effect decreased with decreasing size for all conditions. The spacing required to reduce the effect of insitu ratio was higher for higher insitu ratios.

**Arora et al. (1987)**

They carried out triaxial and uniaxial tests on different rock specimens of Plaster of Paris, Jamrani Sandstone and Agra Sandstone. The rock specimens consisted of different jointed models with varying number of joints and varying number of angles. Based on the experimental results, a parameter called joint factor was proposed which is uniquely related to the ratio of uniaxial compressive strength of the jointed rock model to the uniaxial compressive strength of the intact rock and also to the ratio of elasic modulus of jointed rock model to the elastic modulus of the intact rock.

**Tiwari et al. (2005)**

They carried on triaxial testing on different jointed rock models and determined their post failure behaviour. The testing was performed on True Triaxial System (TTS) which itself was developed by them. The testing was carried on using sand lime models. Using the joint geometry and stress conditions, a zonation table was proposed for assessing strain hardening, softening and plasticity behaviour of the rock . Also, expressions are suggested to estimate postpeak modulus in different triaxial conitions.

**Elsayed (2011)**

He investigated the effect of different parameters such as nature of rock and thickness of shotcrete considering a particular model of tunnel system using Finite Element Method. Also, the analysis was made before and after activation of shotcrete lining. Based on the results, the thickness of lining required for the the tunnels of different rock materials were predicted.

**Raghavendra et al. (2015)**

They carried out the elasto-plastic analysis of twin-tunnel system when subjected to the conditions of gravity, hydrostatic pressure combined with blast induced pressures. The effect on neighbouring tunnels was studied. Also, the effect was considered in the presence and absence of tunnel support systems. The modelling and analysis was carried out using Ansys.

# CHAPTER 3

# MATERIAL CHARACTERIZATION

# EXPERIMENTAL WORK AND METHODOLOGY

A proper understanding of quality of rock mass is necessary for a better and safe design of civil and mining structures on or in rocks. Mechanical and physical properties of the rocks are required to be evaluated for assessing the rock quality. The compositional, physical and geotechnical properties of Schist rocks are studied by carrying out different experiments and are presented below

## MATERIAL AND METHODS

The material used for the study is Schist Rock. The Rock Samples are brought from the Mines in Jalda area of Rourkela which is 30km from NIT Rourkela.


**Figure 3.1 : Location of site from where rock samples have been brought**

## SCANNING ELECTRON MICROSCOPE TEST

The morphology and elemental composition of the rock was studied using Scanning Electron Microscope. The images are produced by scanning the sample with focused beam of electrons. The various signals that are produced due to interaction of the electrons with the atoms in the sample are detected. These contain data about the Microscopic Structure and Elemental Composition of the sample.

The different apparatus used can be shown by the following images. Initially, the sample is made suitable for the test by using the apparatus as shown in Figure by making it to be of conducting nature. Thereafter, the test is conducted using the obtained sample using the apparatus as shown in Figure 3.2.

(a)


(b)

**Figures 3.2 (a), (b) : Apparatus used for Scanning Electron Microscope**

## X-RAY DIFFRACTION TEST

The X-Ray Diffractometer works on the principle that X-Ray beams diffracted are characteristics of the different mineral groups present in the sample. The mineralogical composition of the rock was studied using X-Ray Diffractometer which is shown in Figure . Fine grained powder of the rock sample was made to undergo the test as shown in Figure 3.3.


(a)

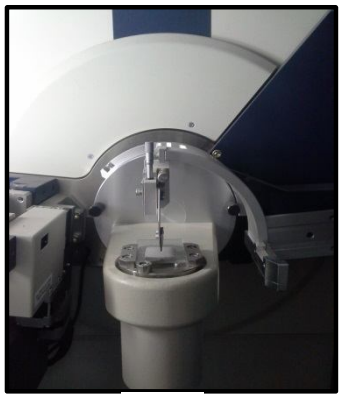

(b)

**Figures 3.3 (a) : Apparatus used for X-Ray Diffraction Test (b) : Specimen undergoing X-Ray Diffraction Test**

## PROTODYAKONOV TEST

The Protodyakonov Strength Index obtained from this test is used to characterize rock mass strength and its brittleness. The rock sample is initially made to pass through a Jaw Crusher (as shown in Figure) followed by rigorous hammering. Then, 100gms of rock pieces of size ranging between 3.35-4.75mm is collected (as shown in Figure) which is used as specimen for the test. The prepared rock specimen is taken in a vertical cylinder with an attached steel plunger as shown in Figure. The plunger is dropped from a height of 65cm for 20 times. The crushed sample is then sieved using 0.5mm sieve. The part of the sample which is passing through the sieve is collected in a Volumeter. The height 'h' in the Volumeter is noted.

Now, the Protodyakonov Strength Index (PSI) is calculated using:

$$PSI = \frac{20n}{h}$$ where n = number of blows = 25

**(a)**

**(b)**

**Specifications**:

**Hollow Cylinder**
Inner Diameter: 78mm
Outer Diameter: 85mm
Height: 763mm

**Steel Plunger**
Diameter: 73mm
Weight: 2.4kg

**(c)**

**(d)**

**Figures 3.4 (a) : Jaw Crusher (b) : Hollow Cylinder and Steel Plunger used for the Protodyakonov Test (c) : Rock Specimen prepared for Protodyakonov Test**

## IMPACT STRENGTH TEST

The Impact Strength Index obtained from this test is another parameter which is used to characterize rock mass strength. This test requires 100gms of rock pieces with size ranging between 3.35-4.75mm as specimen which is same as that of Protodyakonov Test. The prepared rock specimen is taken in a vertical cylinder as shown in Figure . The specimen is subjected to 20 blows of hammer from a height of 30cm. The crushed sample is sieved using a 3mm sieve. The weight of the retained sample (in gms) over the sieve gives the value of Impact Strength Index.

**Specifications:**

**Hollow Cylinder**
**Inner Diameter: 78mm**
**Outer Diameter: 85mm**
**Height: 763mm**

**Steel Plunger**
**Diameter: 44mm**
**Weight: 1.8kg**

**Figure 3.5 : Hollow Cylinder and Steel Cylinder used for Impact Strength Test**

## SLAKE DURABILITY TEST

This test is carried out as per the specifications of IS 10050 – 2001. The schematic diagram of the apparatus used is as shown in Figure 3.6b . The specimen required for this test consists of total mass of 1kg of rock samples with each rock piece of 50±5gms. The prepared rock specimen is as shown in Figure 3.6a . The Slake Durability Test is carried out in two cycles for the prepared rock specimen and corresponding Slake Durability Indices are obtained.

The different labelled parts of the apparatus are as follows:

1. Motor Box
2. Water Tank
3. Brass Drum
4. Wooden Base
5. Switch
6. Timer
7. Coupling

(a)

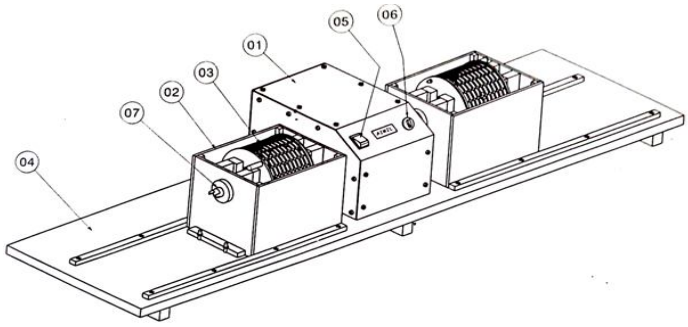


(b)

**Figures 3.6 (a) : Rock Specimen prepared for Slake Durability Test (b) : Apparatus used for Slake Durability Test**

## LOS ANGELES ABRASION TEST

This test is carried out as per the specifications of ASTM : C535. The apparatus used for this test is as shown in Figure 3.7c . The specimen required for this test consists of rock pieces of size ranging between 37.5-50mm with a total mass of 5kg. The abrasive charge used is as shown in Figure 3.7b . The rock specimen along with the abrasive charge is taken in the drum of the apparatus. The testing machine is rotated for 500 revolutions at a speed of 20 rev/min. The rock specimen before and after testing is as shown in Figures 3.7c and 3.7d. Then, the mass of the rock specimen coarser than 1.7mm is measured and Los Angeles Abrasion value is calculated.

**(a) : Specifications of Drum**

**Diameter: 700mm**
**Length: 500mm**

**(b) : 12 Iron Spheres**

**Diameter: 48mm**
**Mass: 400g**

**(c) : Before Testing**

**37.5 to 50mm sized sample**

**(d) : After Testing**

**1.7 to 50mm sized sample**

**Figures 3.7 (a) : Apparatus used for Los Angeles Abrasion Test (b): Abrasive Charge (c), (d) : Rock Specimen before and after the Los Angeles Abrasion Test**

## SCHMIDTH REBOUND HAMMER TEST

This test is carried out as per the specifications of IS 12608 : 205. This is an indirect method for finding out the Uniaxial Compressive Strength of rock. This is used for quick measurement and for insitu measurement. The Schmidth Rebound Hammer used is as shown in Figure 3.8. The Schmidth Rebound Hardness is noted when pressed against the sample at an angle of 45º above and below horizontal. The readings are taken for 20 different points. The average value is then taken as the Schmidth Rebound Hardness and the corresponding Uniaxial Compressive Strength is found out from the chart.

**Figure 3.8 : Schmidth Rebound Hammer Test Apparatus**

## ROCK CORE SPECIMEN PREPARATION

Major of the rock experiments involve cylindrical rock cores of required diameter and length. Rock core preparation is a very rigorous process which involves

Coring, Grinding and Lapping. Coring involves drilling of the rock sample using a rock coring equipment to extract the cylindrical rock core. Grinding involves cutting of the rock core using the grinder equipment to get the required length. Lapping involves polishing of the end surfaces of the rock core specimen by rubbing the end surfaces against Corundum powder.

The different processes of rock core specimen preparation can be as shown in the Figure 3.9.

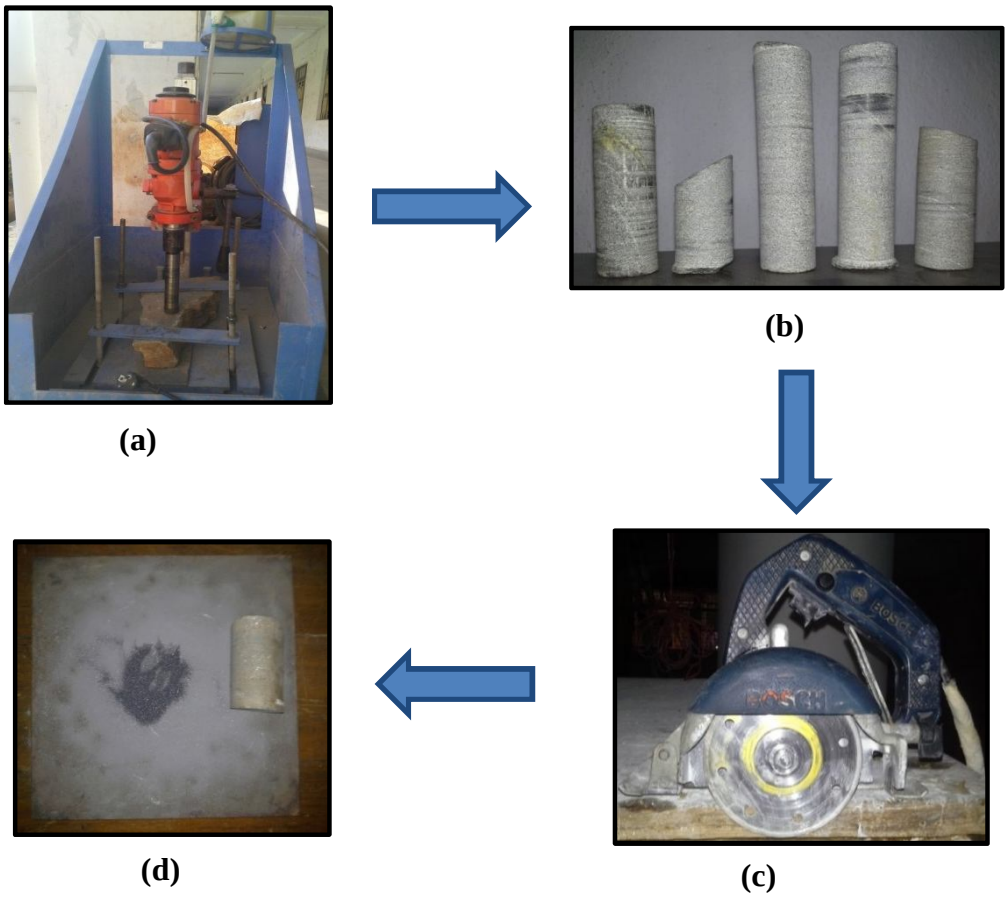


**Figures 3.9 (a) : Rock Coring Apparatus (b) : Obtained Rock Cores after rock coring (c) : Rock Cutting Machine (d) : Lapping using Corundum powder**

## BRINNEL HARDNESS TEST

This test is carried as per the specifications of ASTM : E10. The apparatus used for this test is as shown in Figure . The prepared specimen are cylindrical rock cores of diameter 54mm and thickness 18mm as shown in Figure 3.10. The indenter is

brought into contact with the end surface of the specimen by placing it in the apparatus as shown. A force of 500kgf is applied for a period of 30s and then removed. The microscopic view of the indentation as taken through a microscope is as shown in Figure 3.10b. The diameter of the circular indentation is measured using the microscope which is attached to a millimetre scale. The Brinnel Hardness value is now obtained from the chart by matching with the applied force and the corresponding diameter of the indentation.

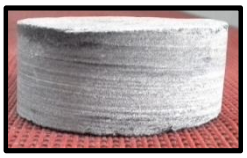

**Diameter 54mm**
**Thickness 18mm**

**(a)**

**(b)**

**(c)**

**Figures 3.10 (a) : Rock Specimen prepared for Brinnel Hardness Test (b) : Microscopic view of the indentation formed (c) : Brinnel Hardness Tester Apparatus**

## BRAZILIAN TENSILE TEST

This test is carried out as per the specifications of IS 10082 : 2001. The apparatus used for this test is as shown in Figure 3.11b. The prepared specimens are cylindrical rock cores of diameter 54mm and length 27mm as shown in Figure 3.11a. The loading is applied diametrically as shown and increased gradually. The loading corresponding to the failure of the rock core is noted and the corresponding tensile strength of the rock is calculated.

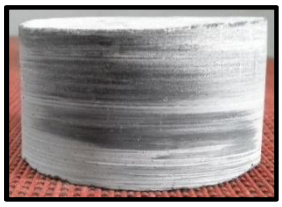

Diameter 54mm

$\frac{L}{D} = 0.5$

**(a)**

**(b)**

**Figures 3.11 (a) : Rock Specimen prepared for the Brazilian Tensile Test**
**(b) : Brazilian Tensile Test apparatus**

## IZOD PENDULUM IMPACT TEST

This test is carried out as per the specifications of ASTM : D256. The apparatus used for this test is as shown in Figure 3.12b. The prepared specimens are thin rock bars of dimensions 85mm x 20mm x 5mm with the notch at a distance of 20mm from the longitudinal end as shown in the Figure 3.12b. The pendulum is dropped from a particular height with the specimen bars in the holder. Thereby, the corresponding reading is noted and izod impact resistance is calculated.

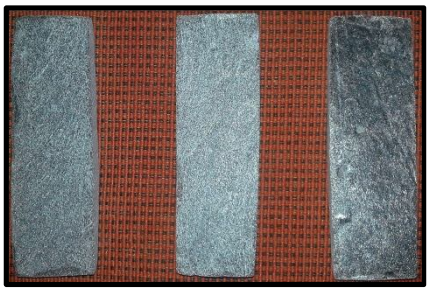

**(a)**


**(b)**

**Figures 3.12 (a) : Rock Specimens prepared for Izod Pendulum Impact Test**
**(b) : Izod Pendulum Imact Testing apparatus**

## POINT LOAD STRENGTH TEST

This test is carried out as per the specifications of IS 8764 : 2003. The apparatus used for this test is as shown in Figure 3.13a. This test is conducted for the different cases which are (a) Irregular Specimen (as shown in Figure 3.13b) (b) Axial Test(as shown in Figure 3.13c) (c) Diametrical Test(as shown in Figure 3.13d).

In the Axial Test, the loading is applied axially on the prepared specimen as shown in Figure . In the Diametrical Test, the loading is applied diametrically on the specimen as shown in the Figure . In all the cases, the loading is gradually increased till the specimen fails. The corresponding load at the point of failure is noted and the Point Load Strength Index is calculated.

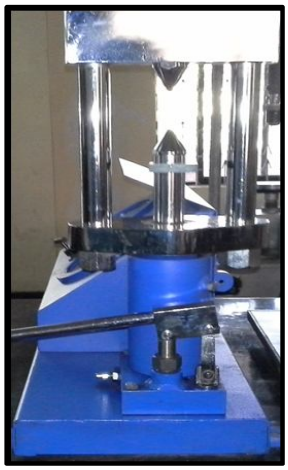

**Irregular Rock Specimen**

**Diameter 54mm**

$\frac{L}{D} = 1$

**Diameter 54mm**

$\frac{L}{D} = 1.5$

**Figures 3.13 (a) : Point Load Strength Index Apparatus (b) : Point Load Strength Index Test for Irregular Rock Specimen (c) : Rock Specimen undergoing Point Load Strength Index Test in Axial position (d) : Rock Specimen undergoing Point Load Strength Index Test in Diametrical position**

## UNIAXIAL COMPRESSIVE STRENGTH TEST

This test is carried out following the specifications as per IS 9221 : 2001. The prepared specimens are cylindrical rock cores of diameter 54mm and $\frac{L}{D} = 2$ as shown in Figure 3.14.


**Figure 3.14 : Rock Specimen prepared for Uniaxial Compressive Test**

## TRIAXIAL COMPRESSIVE STRENGTH TEST

This test is carried out as per the specifications of IS 13047 : 2001. The prepared specimens are cylindrical rock cores of diameter 54mm and $\frac{L}{D} = 2$ which are same as that of Uniaxial Compressive Strength Test. The specimens are tested at confining stresses of 2, 4 and 6 MPa. Thereafter, the cohesion and angle of friction are calculated.

# RESULTS AND DISCUSSION

## SCANNING ELECTRON MICROSCOPE TEST

The images of the Microscopic Structure at different points of the rock sample obtained are as shown in Figure 3.15. From this analysis, the rock sample has **Foliated structure**. Foliated structure means the rock has sheet-like planar structure.

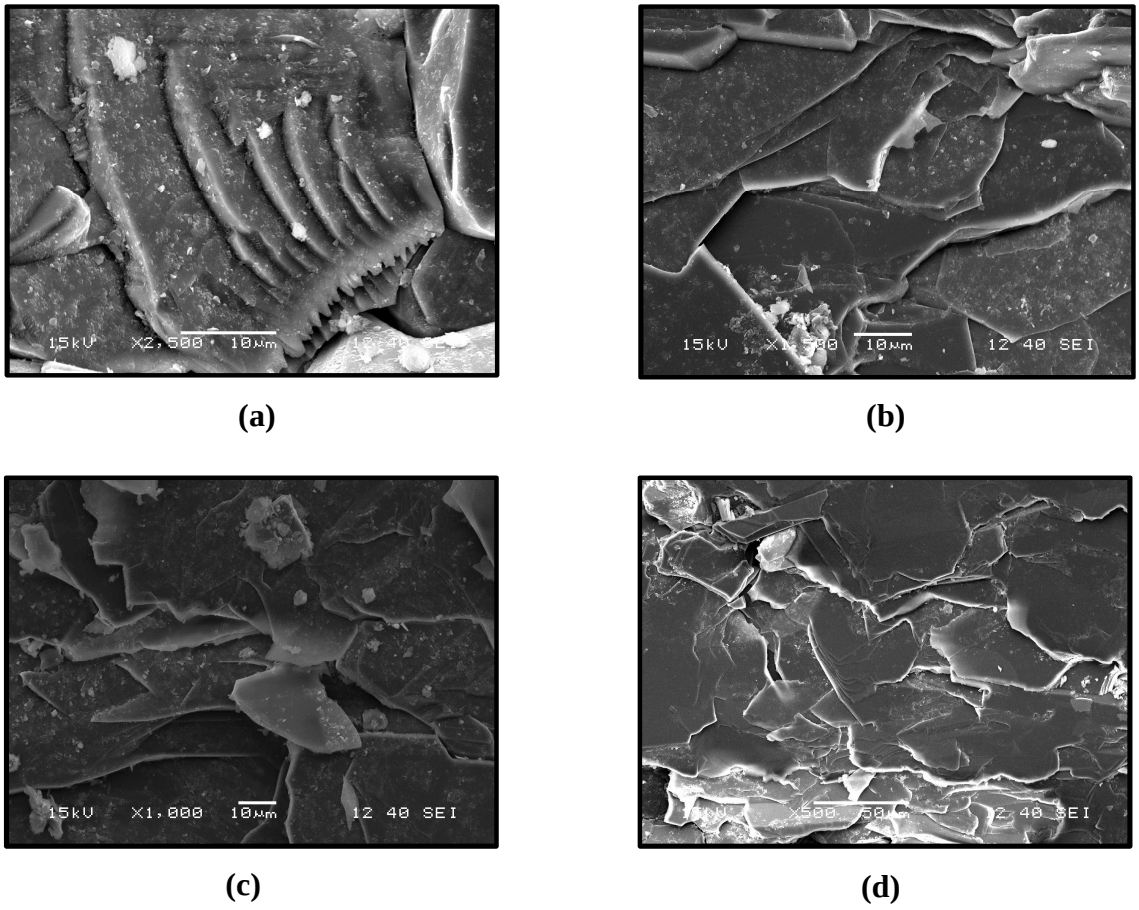


**Figures 3.15 (a), (b), (c), (d) : Microscopic images of the rock specimen obtained from Scanning Electron Microscope**

The Energy Dispersive Spectrum of the sample is as shown in Figure 3.16 and the Elemental composition is as shown in Table 3.1.

| Elements present | Oxygen | Magnesium | Aluminium | Silicon | Potassium | Iron |
|---|---|---|---|---|---|---|
| Weight (in %) | 41 | 2.29 | 15.34 | 24.59 | 5.64 | 11 |

**Table 3.1 : Elemental Composition of the rock specimen**

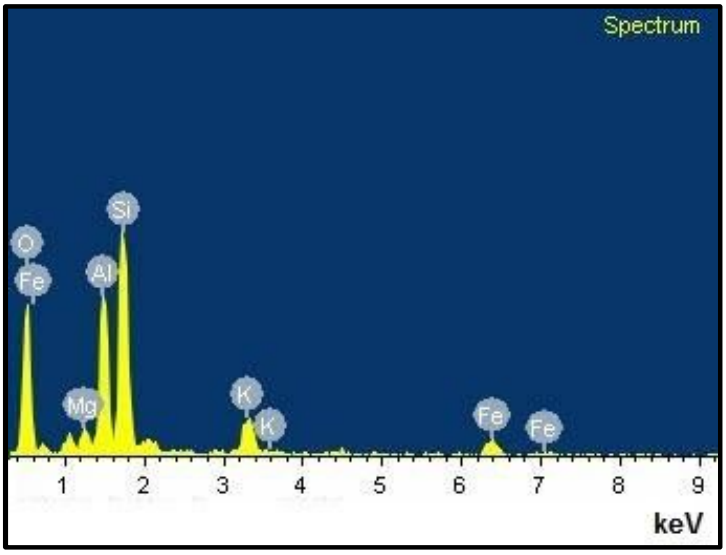


**Figure 3.16 : Energy Dispersive Spectrum of the rock specimen**

## X-RAY DIFFRACTION TEST

The X-Ray Diffraction analysis can be as shown in Figure 3.17.

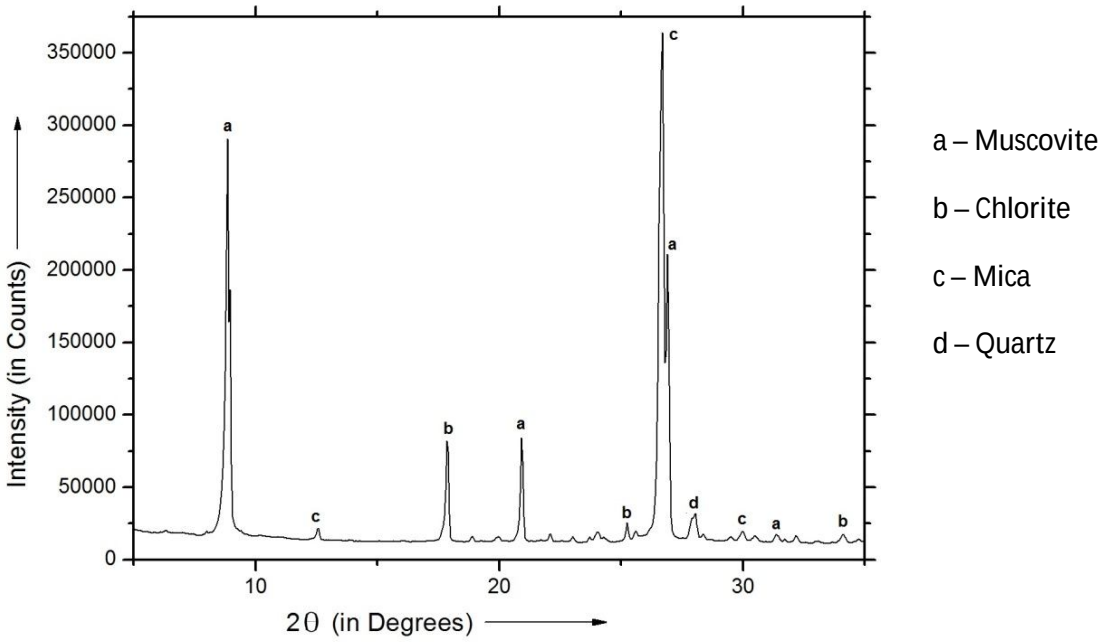


**Figure 3.17 : XRD pattern of the rock specimen**

**Muscovite [$KAl_2(AlSi_3O_{10})(OH)_{10}$]** makes the rock a poor electrical conductor and thermal insulator owing to the presence of its low iron content.

**Chlorite [$Mg_5Al(Si_3Al)O_{10}(OH)_8$]** gives yellowish colour to the rock and makes the rock flexible.

**Mica [$K_{0.974}(Fe_{1.4}Li_{0.75}A_{0.854})(Al_{0.83}Si_{2.85}O_{10})((OH)_{0.94}F_{1.06})$]** gives lustre to the rock and makes the rock more workable.

**Quartz [$SiO_2$]** increases the resistance of the rock to both heat and chemicals. It also makes the rock hard enough so as to prevent it from easily getting crushed. Thus, Quartz makes the rock resistant to weathering.

On the basis of the minerals present in the rock sample, the scientific name is **Muscovite Chlorite Schist**.

## PROTODYAKONOV AND IMPACT STRENGTH TEST

The Protodyakonov Strength Index and Impact Strength Index values of the rock are obtained as **17.64** and **28** respectively.

## SLAKE DURABILITY TEST

The Slake Durability Index values at the end of 1$^{st}$ and 2$^{nd}$ cycles are obtained as 98.83% and 98.73% repectively. Thus, the rocks are **Very High Durable**. This property makes these rocks very much suitable for making breakwaters and other earth works against erosion by water in the form of riprap.

## LOS ANGELES ABRASION TEST

The Los Angeles Abrasion value of the rock is obtained as 20.21%. Thus, the rocks are **very tough** and **can resist wear and tear**. This property makes these rocks very much suitable for putting as ballast to support railway sleepers and as a base, sub-base, top course for roads.

## SCHMIDTH REBOUND HAMMER TEST

The Schmidth Rebound Hardness value of the rock is obtained as **30** and the corresponding Uniaxial Compressive Strength is obtained as 16MPa.

## BRINNEL HARDNESS TEST

The diameter of the indentation formed is 3mm and the corresponding Brinnel Hardness is obtained as **64.6**. From the Brinnel Hardness value, the rock has **less resistance towards indentation**. Thus, the rock can be easily moulded for making monuments and sculptures.

## BRAZILIAN TENSILE TEST

The Tensile Strength of the rock is obtained as **1.18MPa**.

## IZOD PENDULUM IMPACT TEST

The Izod Impact Resistance of the rock is obtained as **392J/m$^2$**. From this value, it can be inferred that the rock can absorb energy when acted upon by large impulses or sudden shocks. This makes the rock suitable to be used for making breakwaters in which the rock masses are subjected to very large impulsive action of the waves of the ocean

## POINT LOAD STRENGTH TEST

The Point Load Strength Index obtained for the different cases of the rock specimen are : (a) **Irregular Specimen – 1.26MPa** (b) **Axial Test – 0.83MPa** (c) **Diametrical Test – 0.81MPa**. This implies that the rock cannot be peeled or scraped with a pocket knife and can be fractured with a single blow of a geological hammer.

## UNIAXIAL COMPRESSIVE STRENGTH TEST

The axial stress and axial strain graph obtained for the rock is as shown in Figure 3.18. The **Ultimate Compressive Strength**, **Elastic Modulus** and **Poisson's ratio** are obtained as **18.56MPa**, **1.64GPa** and **0.19** respectively.

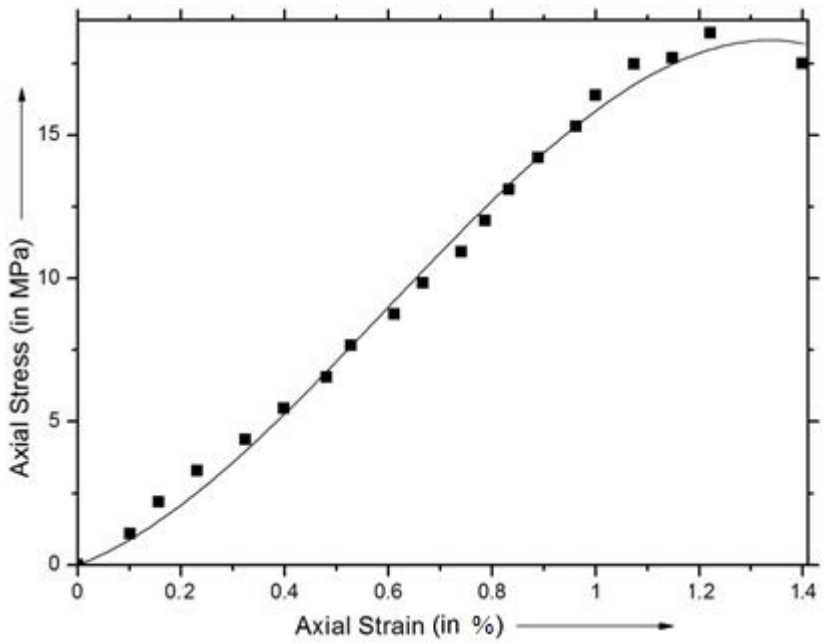


**Figure 3.18 : Stress-strain of the rock specimen obtained from UCS test**

## TRIAXIAL COMPRESSIVE STRENGTH TEST

The Triaxial Compressive Strength test is carried out at confining pressures of 2MPa, 4MPa and 6MPa. The Strength Envelope obtained for the rock is as shown in Figure 3.19. The **Cohesion** and **Angle of Friction** are calculated and obtained as **2.62MPa** and **58.41º** respectively.

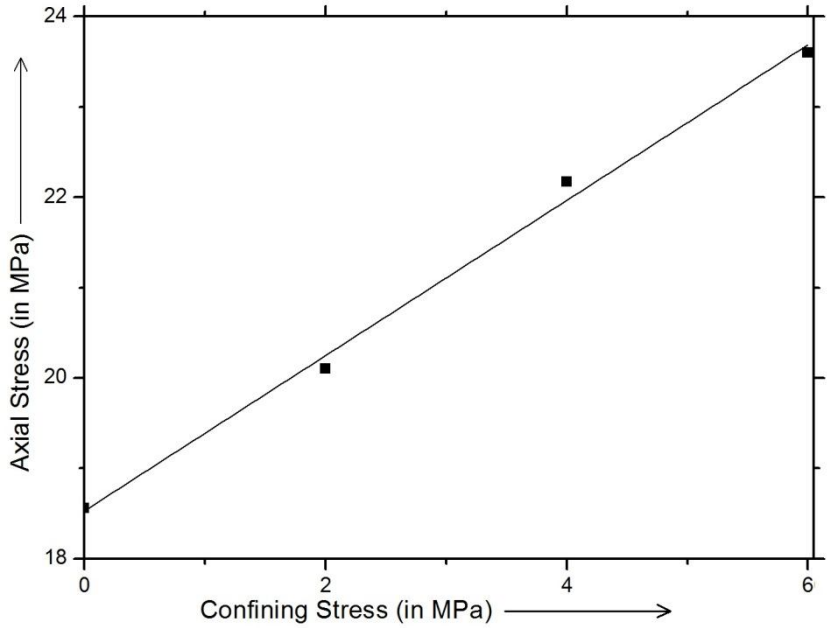


**Figure 3.19 : Strength envelope of the rock specimen obtained from the Triaxial test**

# CHAPTER 4

# STRENGTH BEHAVIOUR OF JOINTED SCHIST ROCK

# THEORY AND METHODOLOGY

Stability of different rock structures such as underground chambers, tunnels, open pits etc. is greatly influenced by the frequency of joints, orientation of joints and the direction of loading. Economical and safe design of these rock structures makes the strength estimation of jointed rock masses very necessary.

Number of joints per unit length, orientation of the joint and shear strength along the joint are major aspects in a rock joint which are measurable and are responsible for the reduction of strength. The joint factor is a simple parameter which is combined suitably for the above three aspects which gives a quantitative measure of the weakness of the rock in comparison to the intact rock. Joint factor can be formulated as:

$$J_f = \frac{J_n}{nr}$$

where $J_n$ is the number of joints per unit length, r is the roughness parameter and n is the inclination parameter which can be obtained from Table 4.1 as suggested by Ramamurthy et al 1994

| Angle of Orientation | 0° | 10° | 20° | 30° | 40° | 50° | 60° | 70° | 80° | 90° |
|---|---|---|---|---|---|---|---|---|---|---|
| Inclination Parameter | 0.82 | 0.46 | 0.11 | 0.05 | 0.09 | 0.30 | 0.46 | 0.64 | 0.82 | 0.95 |

**Table 4.1 : Inclination parameters for different angle of orientations**

Compressive strength ratio of a rock ( $\sigma_{cr}$ ) is the ratio of uniaxial compressive strength of the jointed rock ( $\sigma_{cj}$ ) to that intact rock ( $\sigma_{ci}$ ). Elastic Modular ratio ( $E_{tr}$ ) is the ratio of the tangent modulus of the jointed rock ( $E_{tj}$ ) to that of the intact rock ( $E_{ti}$ ).

$$\sigma_{cr} = \frac{\sigma_{cj}}{\sigma_{ci}} \text{ and } E_{tr} = \frac{E_{tj}}{E_{ti}}$$

Many researchers have developed different correlations for Elastic Modulus ratio and Compressive Strength ratio of the rock to the corresponding Joint factor. Rocks used by different researchers include Granite, Sandstone, Marble, Plaster of

Paris but Schist rock has not been used so far for investigation of its jointed behaviour. In the current experimental study, different jointed rock models of Schist rocks are prepared with increasing number of joints and joint orientation. These specimens are made to undergo uniaxial compressive test with membranes around the cylindrical jointed specimens so as to prevent the sliding along the joint. Thereafter, the obtained results are used for developing correlation for Elastic Modulus ratio and Compressive Strength ratio of Schist rock.

The models of the different jointed rock specimens prepared are as follows:

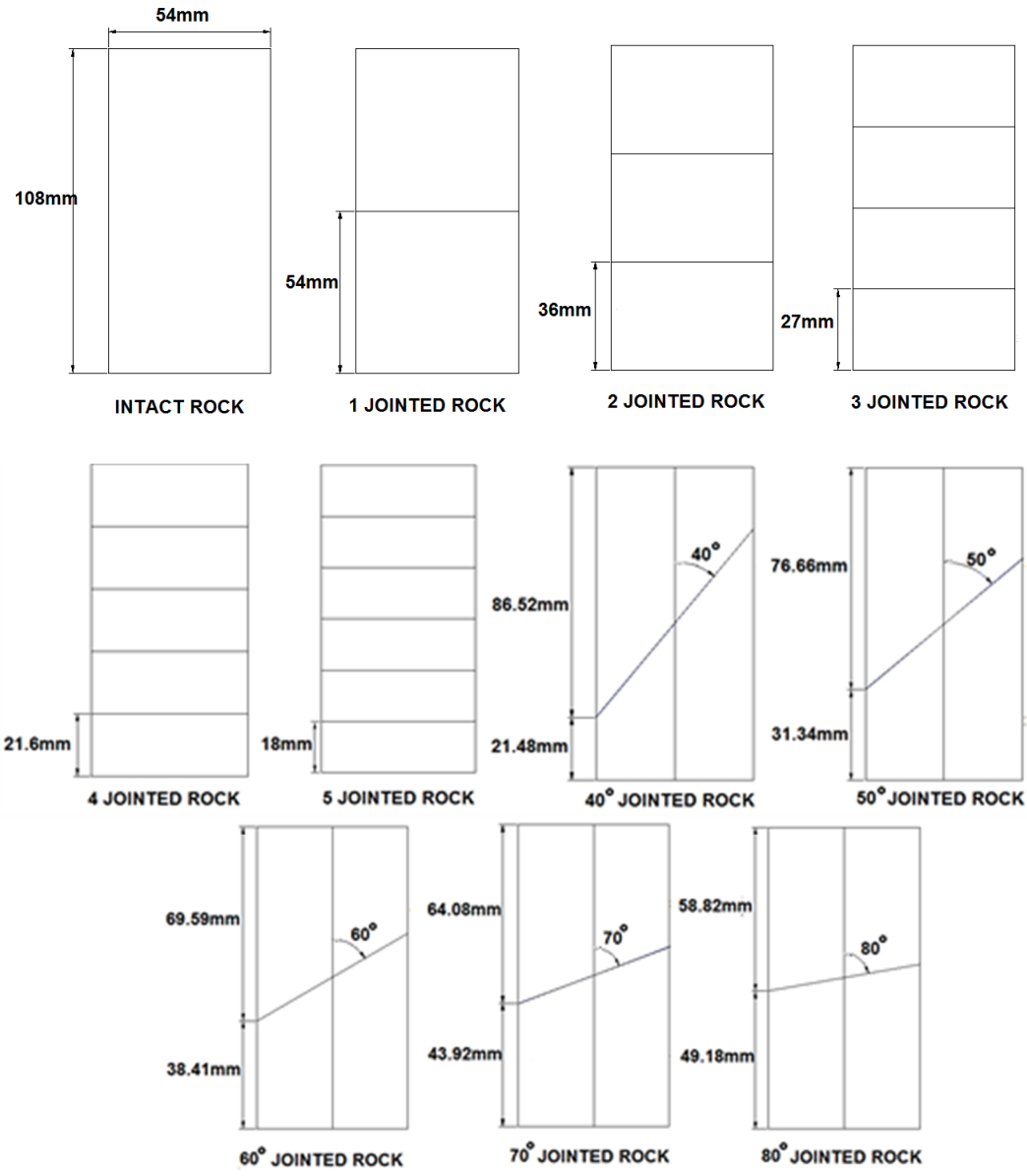


**Figures 4.1 : Different jointed rock models prepared and tested for UCS testing**

# RESULTS AND DISCUSSIONS

The results obtained from the Uniaxial Compressive Strength test of the different jointed schist rock specimens along with the other rock parameters are as follows:

## Intact Rock Specimen

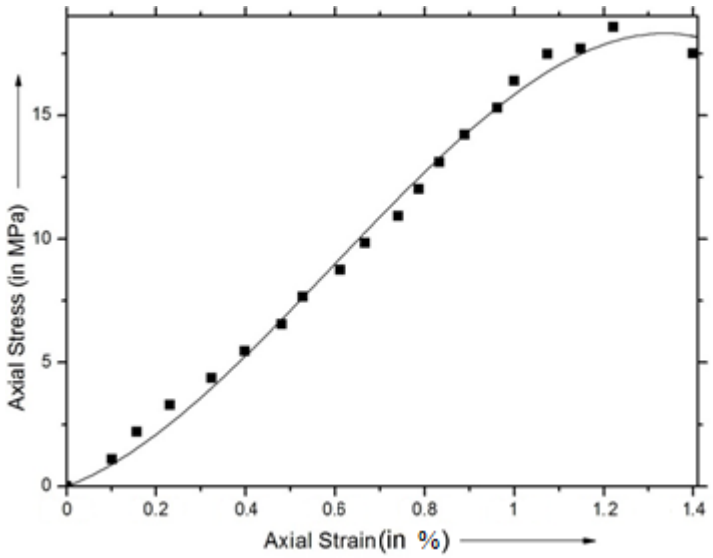


$\sigma_{ci}$ = 18.56MPa
$E_{ti}$ = 1.64GPa
$\sigma_{cr}$ = 1
$E_{tr}$ = 1
$J_f$ = 0

**Figure 4.2 : Stress-strain curve for intact rock specimen from UCS test**

## Rock Specimen with 1 Joint

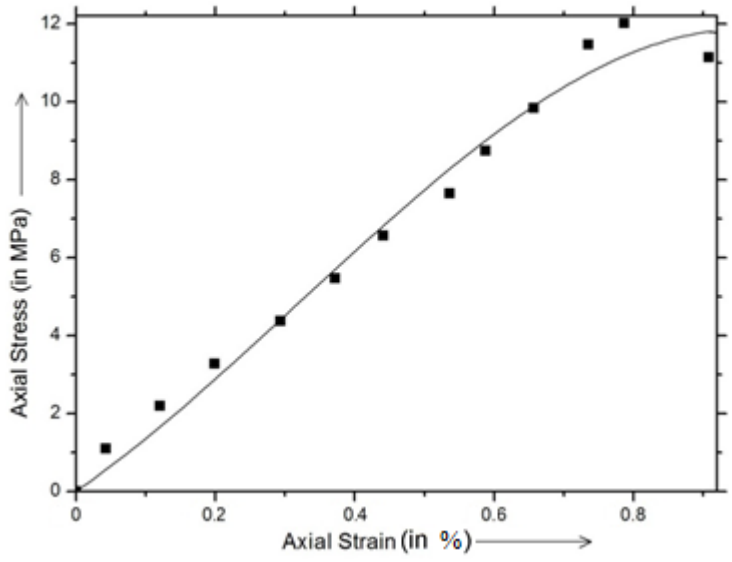


$\sigma_{cj}$ = 12.01MPa
$E_{tj}$ = 1.52GPa
$\sigma_{cr}$ = 0.65
$E_{tr}$ = 0.92
$J_f$ = 6.52

**Figure 4.3 : Stress-strain curve for rock specimen with 1 joint from UCS test**

## Rock Specimen with 2 Joints

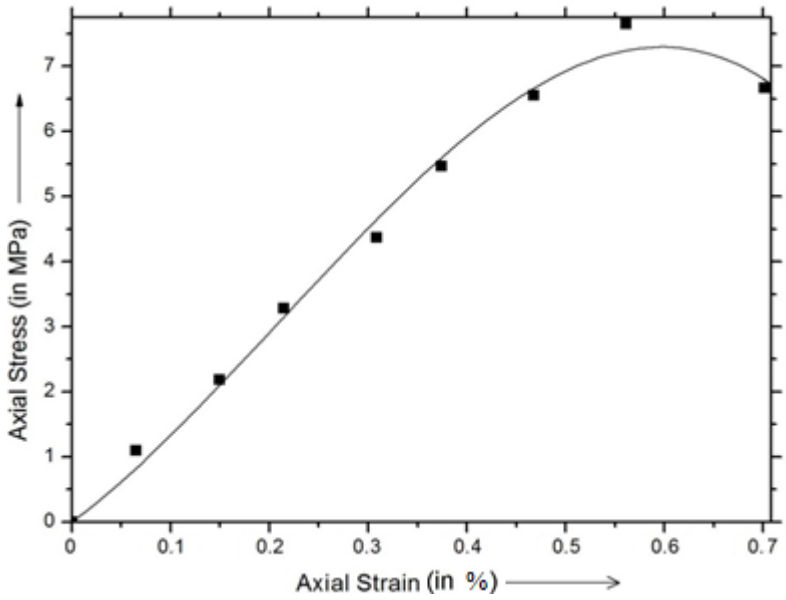


$\sigma_{cj}$ = 7.64MPa
$E_{tj}$ = 1.40GPa
$\sigma_{cr}$ = 0.41
$E_{tr}$ = 0.86
$J_f$ = 13.04

**Figure 4.4 : Stress-strain curve for rock specimen with 2 joints from UCS test**

## Rock Specimen with 3 Joints

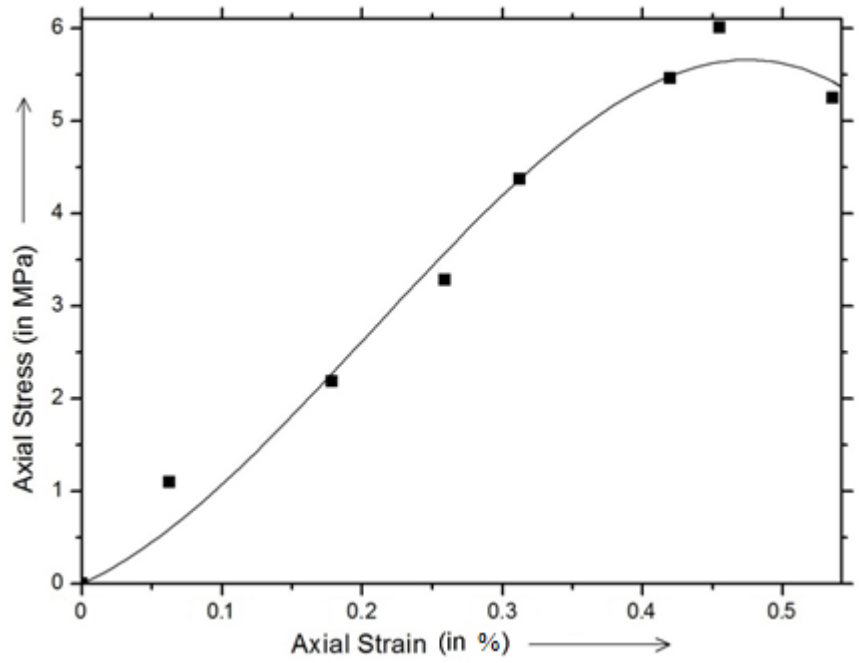


$\sigma_{cj}$ = 6.01MPa
$E_{tj}$ = 1.31GPa
$\sigma_{cr}$ = 0.32
$E_{tr}$ = 0.80
$J_f$ = 19.56

**Figure 4.5 : Stress-strain curve for rock specimen with 3 joints from UCS test**

## Rock Specimen with 4 Joints

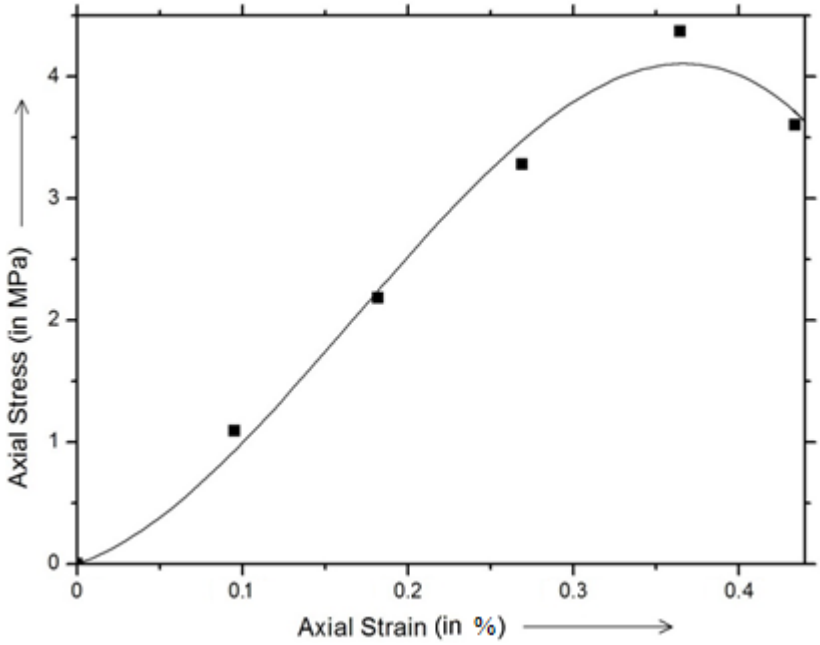


$\sigma_{cj}$ = 4.37MPa
$E_{tj}$ = 1.20GPa
$\sigma_{cr}$ = 0.23
$E_{tr}$ = 0.73
$J_f$ = 26.81

**Figure 4.6 : Stress-strain curve for rock specimen with 4 joints from UCS test**

## Rock Specimen with 5 Joints

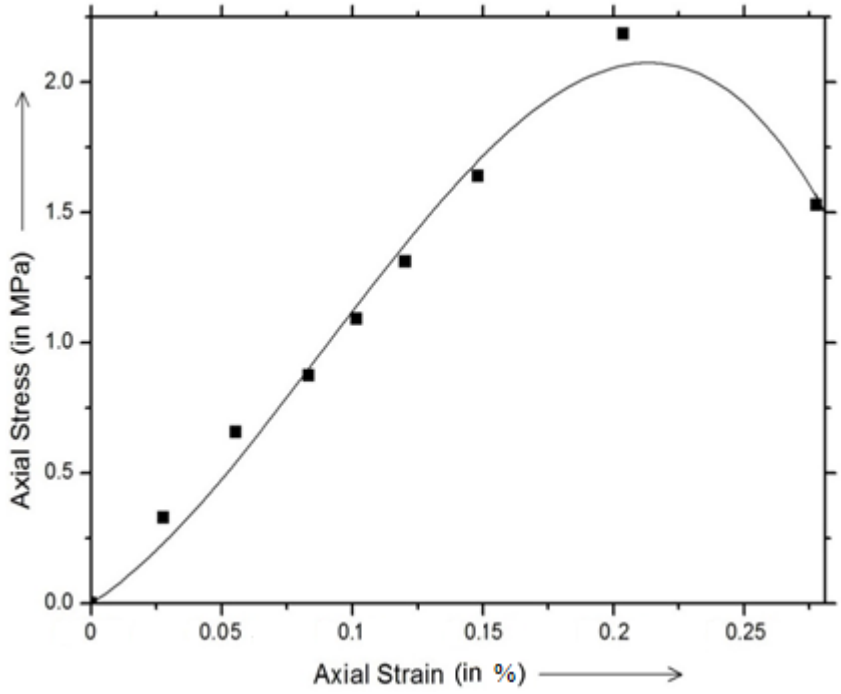


$\sigma_{cj}$ = 2.18MPa
$E_{tj}$ = 1.08GPa
$\sigma_{cr}$ = 0.12
$E_{tr}$ = 0.66
$J_f$ = 33.33

**Figure 4.7 : Stress-strain curve for rock specimen with 5 joints from UCS test**

## Rock Specimen with Joint Orientation 40°

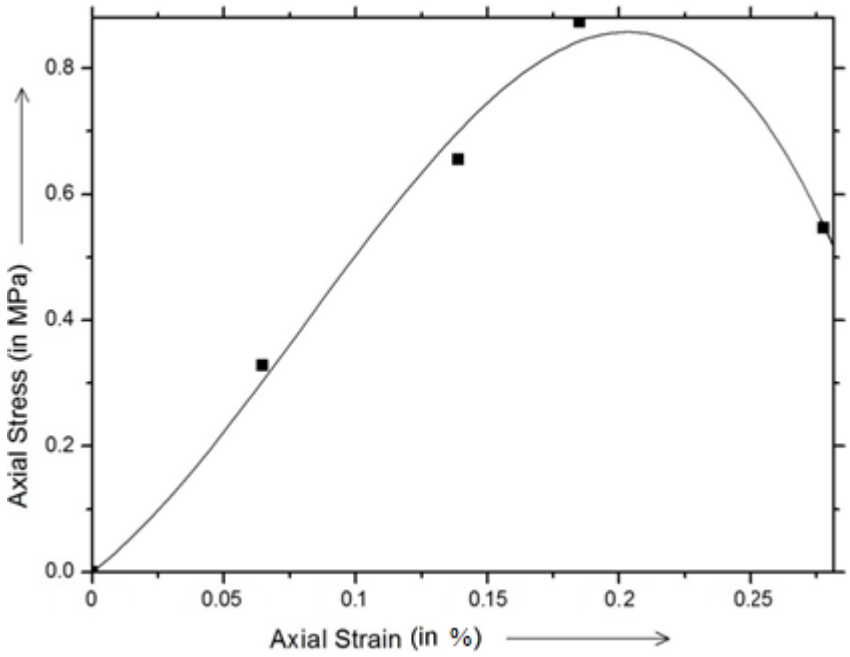


$\sigma_{cj}$ = 0.87MPa
$E_{tj}$ = 0.47GPa
$\sigma_{cr}$ = 0.05
$E_{tr}$ = 0.29
$J_f$ = 91.85

**Figure 4.8 : Stress-strain curve for rock specimen of joint orientation 40º from UCS test**

## Rock Specimen with Joint Orientation 50°

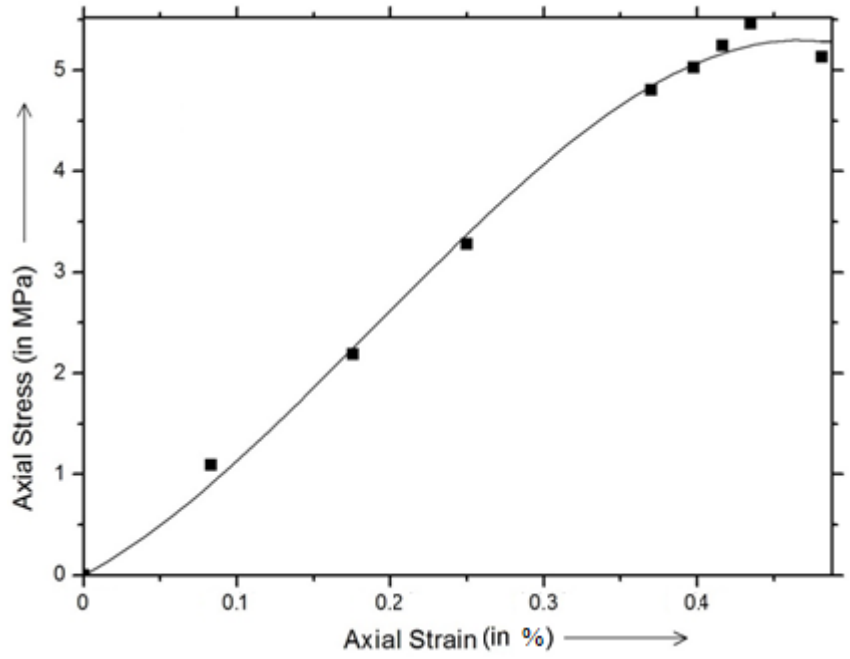


$\sigma_{cj}$ = 5.46MPa
$E_{tj}$ = 1.27GPa
$\sigma_{cr}$ = 0.29
$E_{tr}$ = 0.77
$J_f$ = 21.31

**Figure 4.9 : Stress-strain curve for rock specimen of joint orientation 50º from UCS test**

## Rock Specimen with Joint Orientation 60°

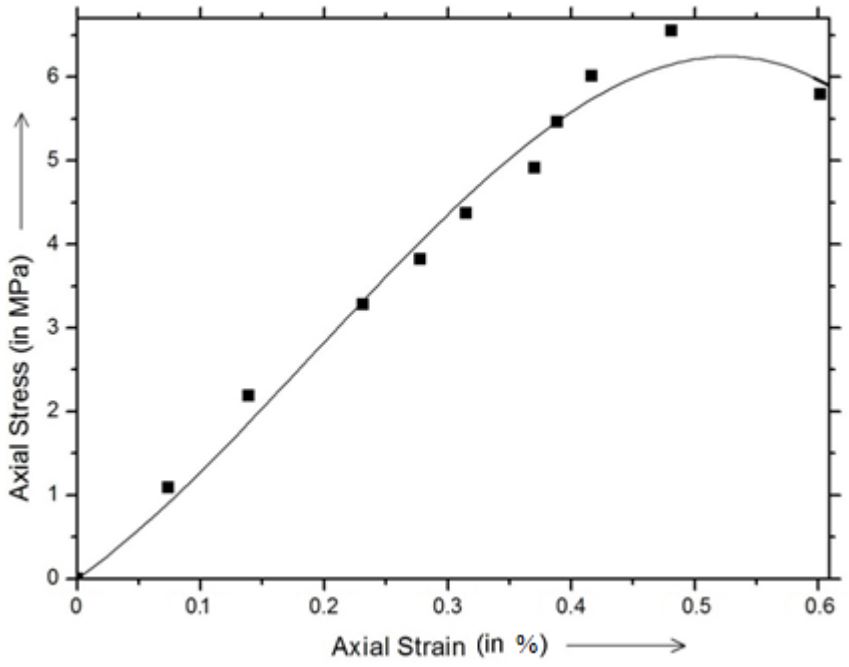


$\sigma_{cj}$ = 6.55MPa
$E_{tj}$ = 1.38GPa
$\sigma_{cr}$ = 0.35
$E_{tr}$ = 0.85
$J_f$ = 14.02

**Figure 4.10 : Stress-strain curve for rock specimen of joint orientation 60º from UCS test**

## Rock Specimen with Joint Orientation 70°

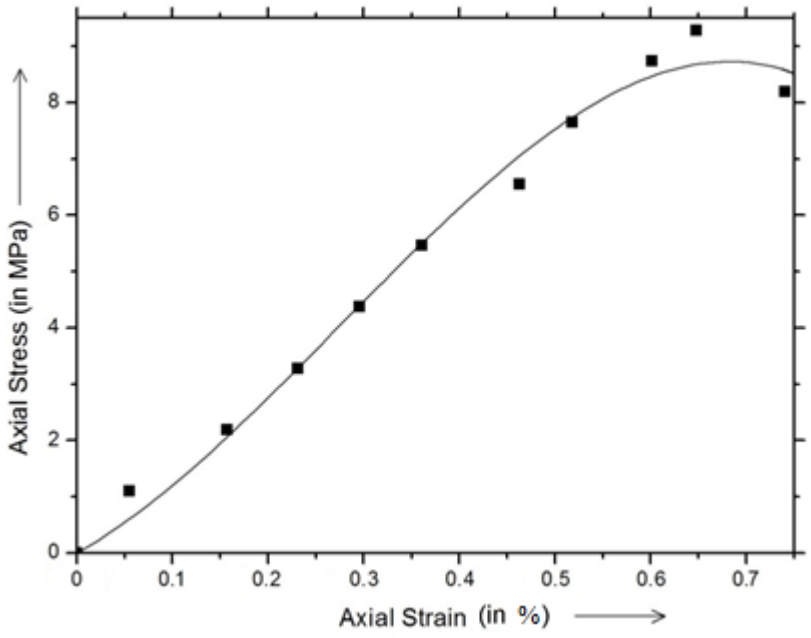


$\sigma_{cj}$ = 9.28MPa
$E_{tj}$ = 1.45GPa
$\sigma_{cr}$ = 0.5
$E_{tr}$ = 0.88
$J_f$ = 10.28

**Figure 4.11 : Stress-strain curve for rock specimen of joint orientation 70º from UCS test**

## Rock Specimen with Joint Orientation 80°

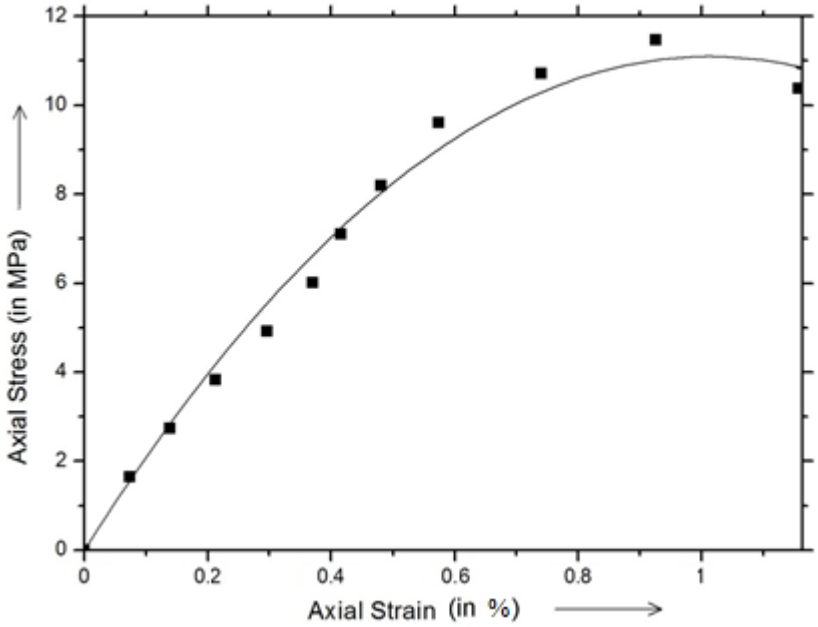


$\sigma_{cj}$ = 11.46MPa
$E_{tj}$ = 1.48GPa
$\sigma_{cr}$ = 0.62
$E_{tr}$ = 0.9
$J_f$ = 8.01

**Figure 4.12 : Stress-strain curve for rock specimen of joint orientation 80º from UCS test**

From the above results, it can be observed that Compressive Strength decreases with the increase in number of joints per unit length. Also, the Compressive Strength decreases with increase in the angle up to a certain angle and then increases.

The $\sigma_{cr}$ and $E_{tr}$ values are obtained as shown in the above Figures by carrying out Uniaxial Compressive tests on the different jointed rock specimens. By using Exponential Regression Analysis, these values are correlated to $J_f$ of the different jointed rock specimens. The correlations can be as shown with the help of Figures .

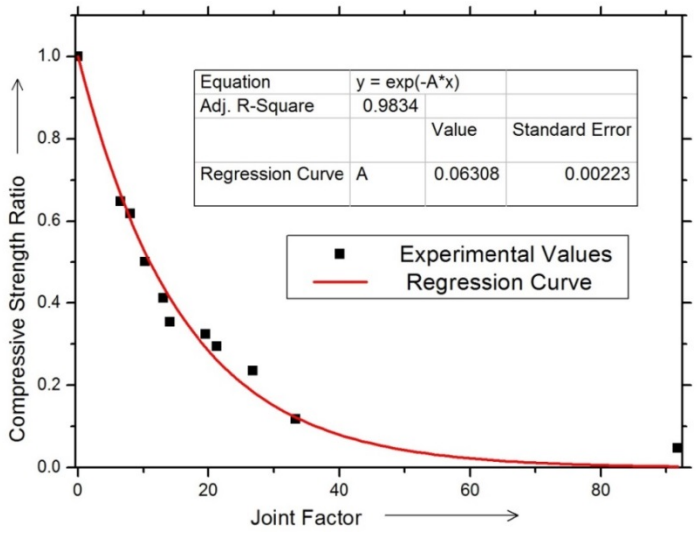


**Figure 4.13 : Correlation between Compressive Strength Ratio and Joint Factor**

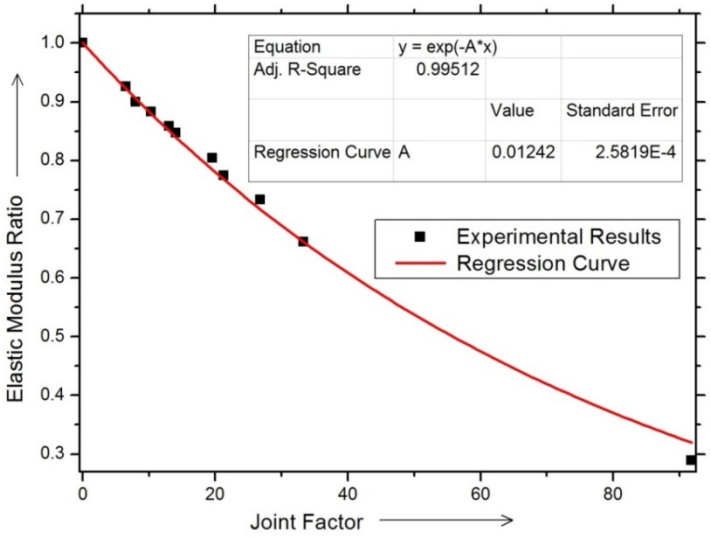


**Figure 4.14 : Correlation between Elastic Modulus Ratio and Joint Factor**

From the Figures, Standard Error and the Adj R-Square values show that the correlations formed are well- fitted with the values of the inputs and outputs. Figures compare the results of the present experimental study with those of work done by other researchers Arora (1987) and Padhy (2005) results.

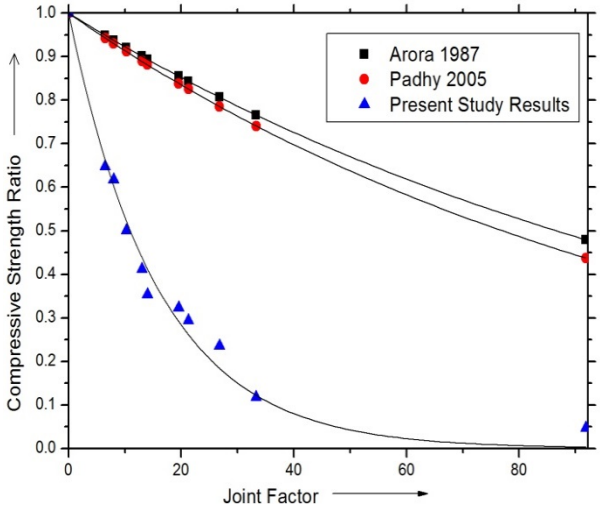


**Figure 4.15 : Comparison of the correlation of Compressive Strength Ratio with others**

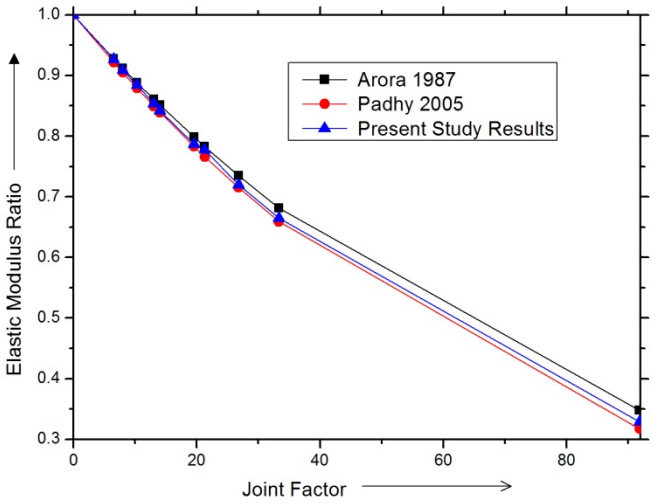


**Figure 4.16 : Comparison of the correlation of Elastic Modulus Ratio with others**

From the above Figures, it can be seen that Elastic Modulus Ratio values are quite closer to that predicted by those of Arora (1987) and Padhy (2005) whereas those of Compressive Strength Ratio are not so closer to that predicted by them.

# CHAPTER 5

# ANALYSIS OF CIRCULAR TUNNELS USING FINITE ELEMENT METHOD

# NUMERICAL MODELING

Realistic analysis of the tunnel behaviour requires a full understanding of the tunnelling procedure to simulate its effects in the analytical model. Simulation requires sufficient representation of the rock characteristics.

In the current investigation, a two-dimensional model of a rock trench with a circular tunnel is considered. A static model is prepared to study the stresses and deformations around a circular tunnel in a rock trench whose properties are those of Schist Rock. Effect of traffic loads above the rock trench and other loads inside the tunnel are neglected as they are insignificant in comparison to the overburden pressure due to the rock mass above the Circular tunnel in the trench. The need of the hour is addressed employing FEM numerical scheme. A finite element model is made for the trench with a circular tunnel using Plaxis 8.2 Professional Version. The trench extends up to a depth of 100m from the ground surface and has a width of 100m. The centre of the tunnel is taken at a depth of 60m from the ground surface. The circular tunnel is analysed for diameters of 5, 10, 15, 20, 25 and 30 metres.

Figure 5.1 shows the two dimensional geometry of the rock trench with a circular tunnel. As a part of pre-processing, the 2D model is discretized into many 15-noded triangular elements. The mesh size is taken as very fine to get the most accurate results. The boundary conditions are defined as shown in the Figure. The sides are given roller support and the bottom is fixed support. Different cases are analyzed with in-situ stress ratios as 0.5, 1 and 1.5 . The different material properties of the rock trench are assigned as obtained from the experimental results which are as shown.

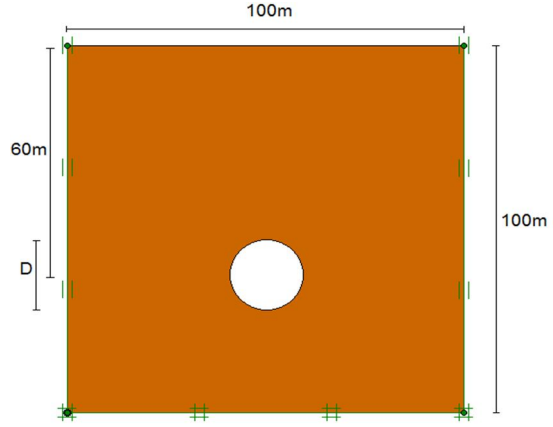


D - Diameter of the Circular Tunnel

| |
|---|
| Dry Density – 26kN/m$^3$ |
| Elastic Modulus – 1.64GPa |
| Poisson's Ratio – 0.19 |
| Shear Modulus – 0.69GPa |
| Cohesion – 2.62MPa |
| Angle of friction – 58.41° |

**Figure 5.1 : Model of the rock trench with the tunnel**

# RESULTS AND DISCUSSIONS

The deformed meshed models, horizontal displacements, vertical displacements, total displacements and stress distributions obtained after solving using Plaxis for the rock trenches with the different diameters of tunnels and insitu stress ratios are as shown.

## INSITU STRESS RATIO 0.5

## CIRCULAR TUNNEL OF DIAMETER 5m

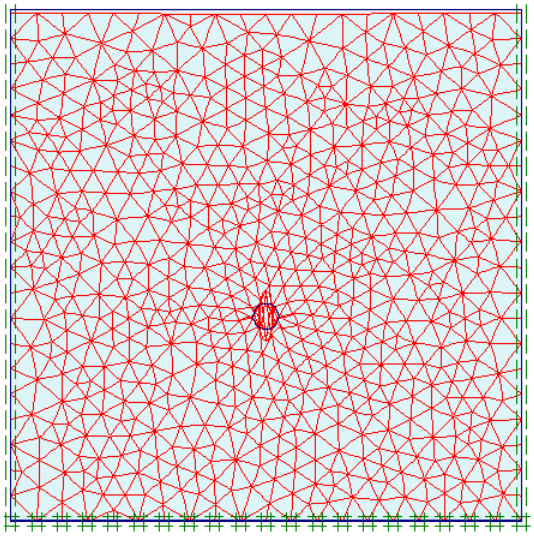

**Figure 5.2 (a)**

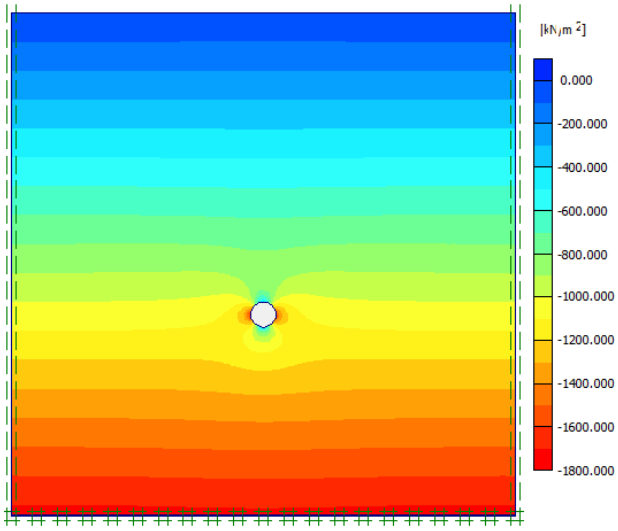


**Figure 5.2 (b)**

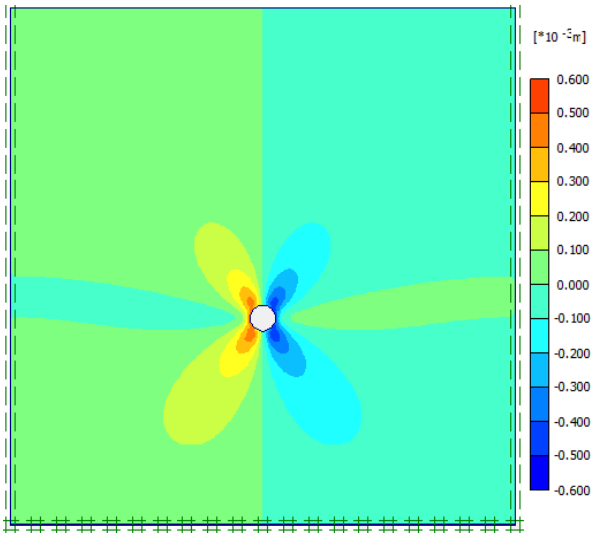


**Figure 5.2 (c)**

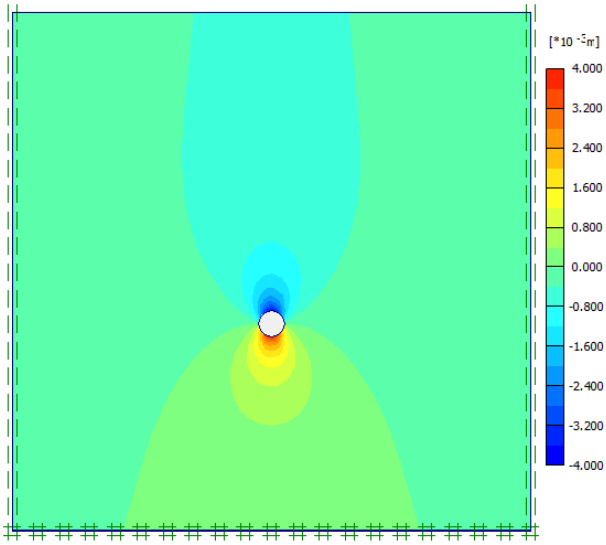


**Figure 5.2 (d)**

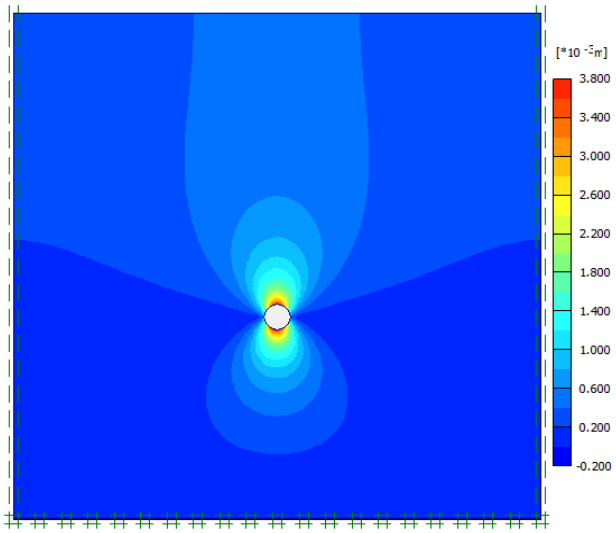


**Figure 5.2 : Tunnel of diameter 5m and insitu stress ratio 0.5 (a): Fine Mesh diagram (b): Stress Contours (c) Horizontal Displacements (d) Vertical Displacements (e) Total Displacements**

**Figure 5.2 (e)**

## CIRCULAR TUNNEL OF DIAMETER 10m

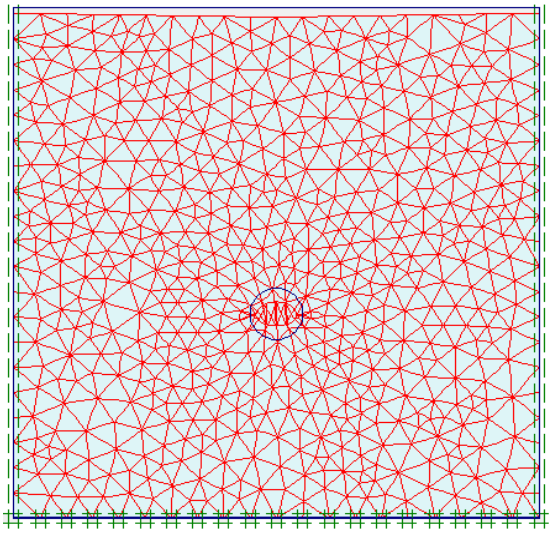

**Figure 5.3 (a)**

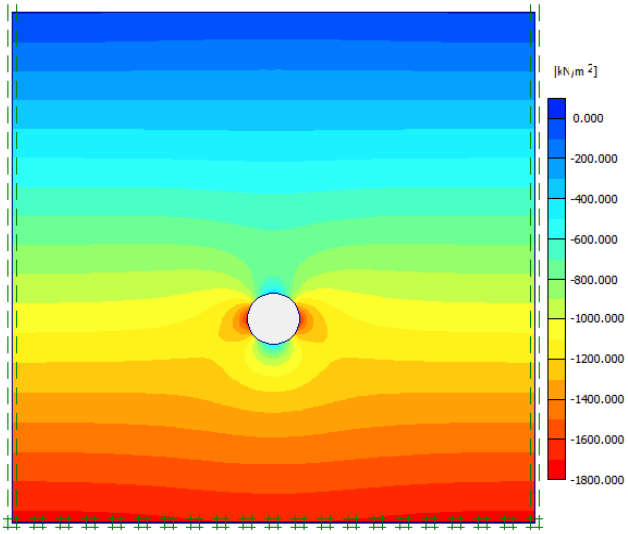


**Figure 5.3 (b)**

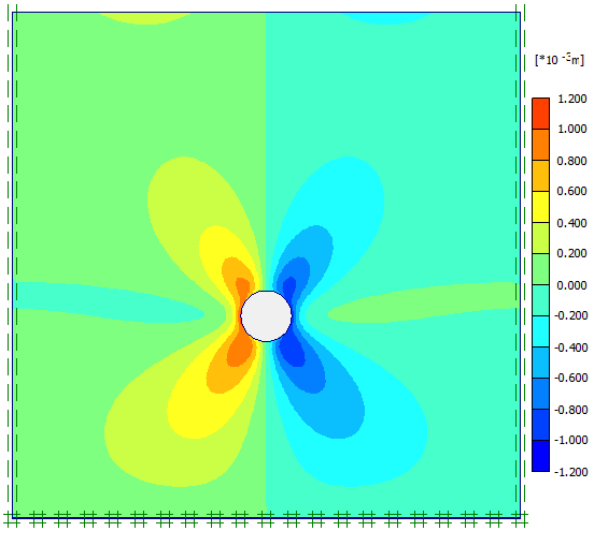


**Figure 5.3 (c)**

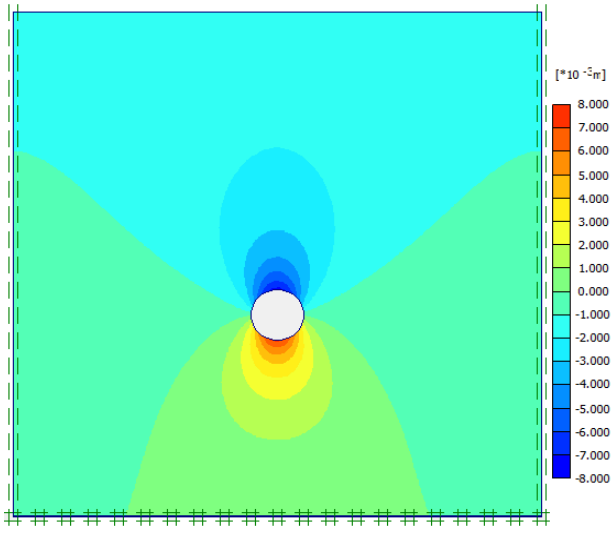


**Figure 5.3 (d)**

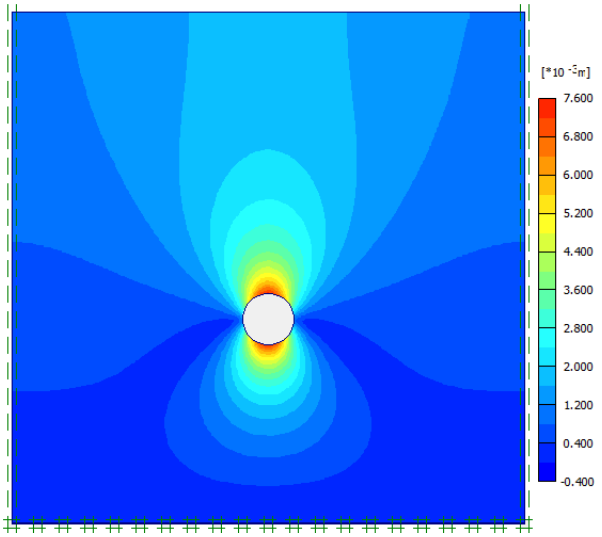


**Figure 5.3 : Tunnel of diameter 10m and insitu stress ratio 0.5 (a): Fine Mesh diagram (b): Stress Contours (c) Horizontal Displacements (d) Vertical Displacements (e) Total Displacements**

**Figure 5.3 (e)**

## CIRCULAR TUNNEL OF DIAMETER 15m

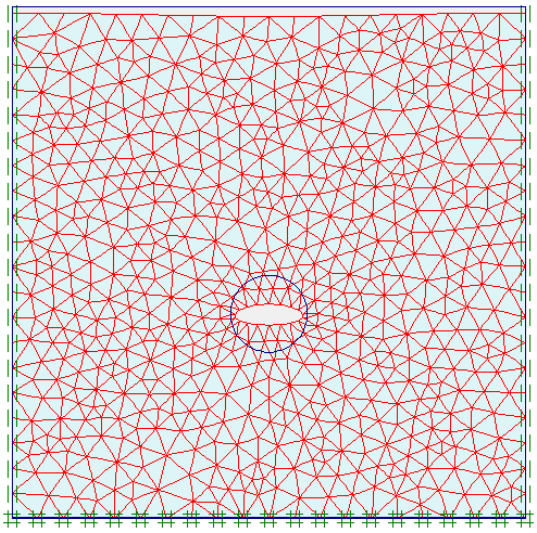

**Figure 5.4 (a)**

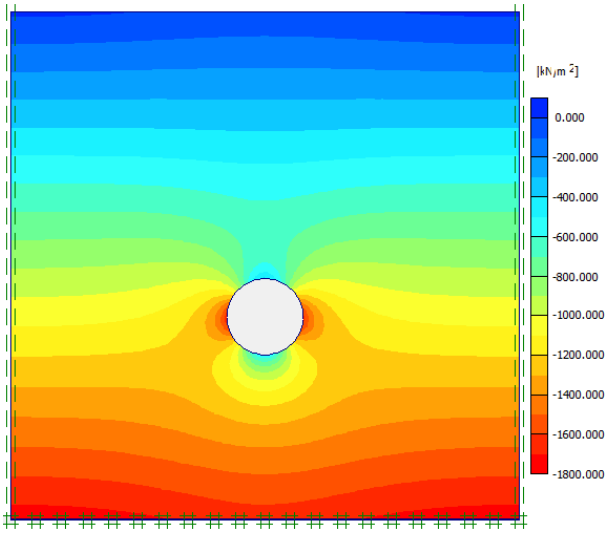


**Figure 5.4 (b)**

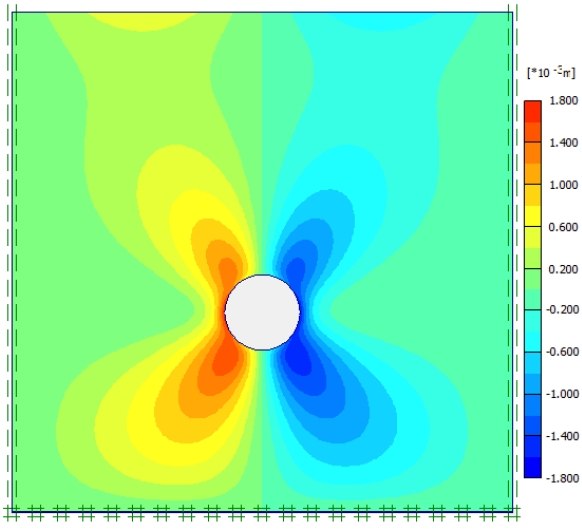


**Figure 5.4 (c)**

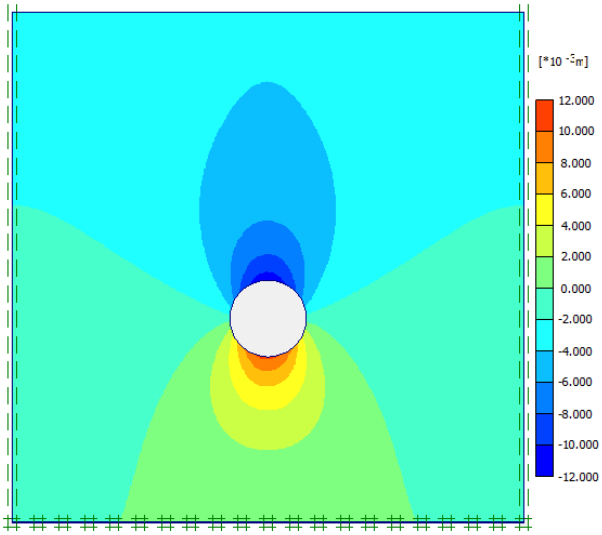


**Figure 5.4 (d)**

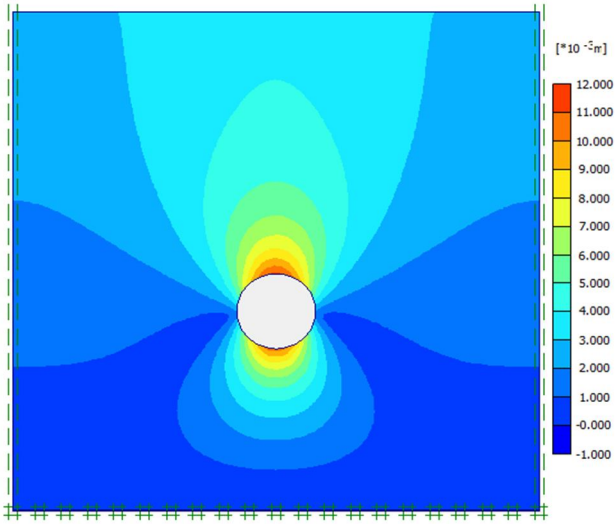


**Figure 5.4 (e)**

**Figure 5.4 : Tunnel of diameter 15m and insitu stress ratio 0.5 (a): Fine Mesh diagram (b): Stress Contours (c) Horizontal Displacements (d) Vertical Displacements (e) Total Displacements**

## CIRCULAR TUNNEL OF DIAMETER 20m

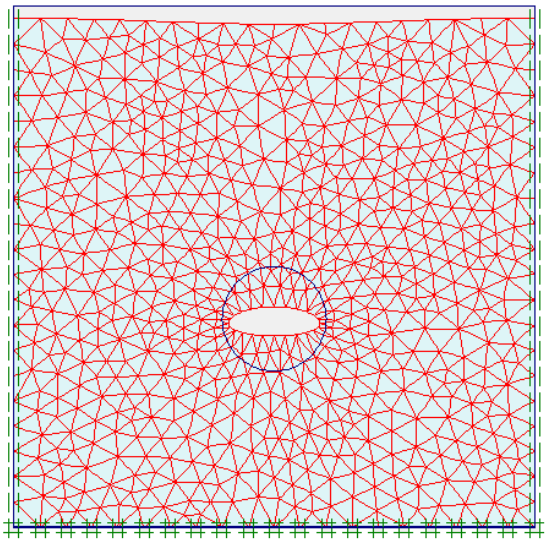

**Figure 5.5 (a)**

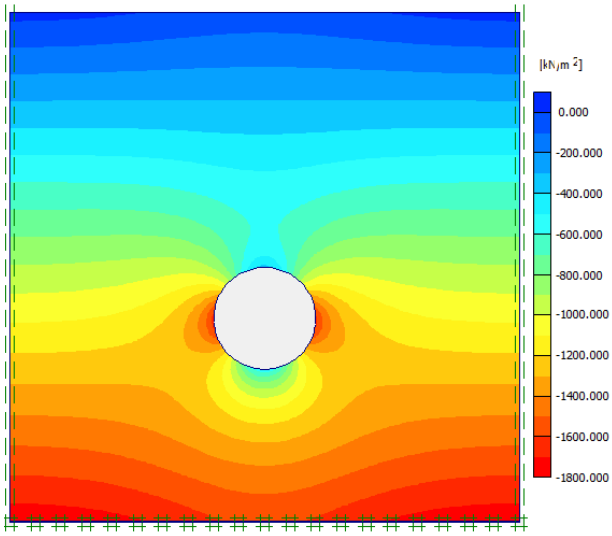


**Figure 5.5 (b)**

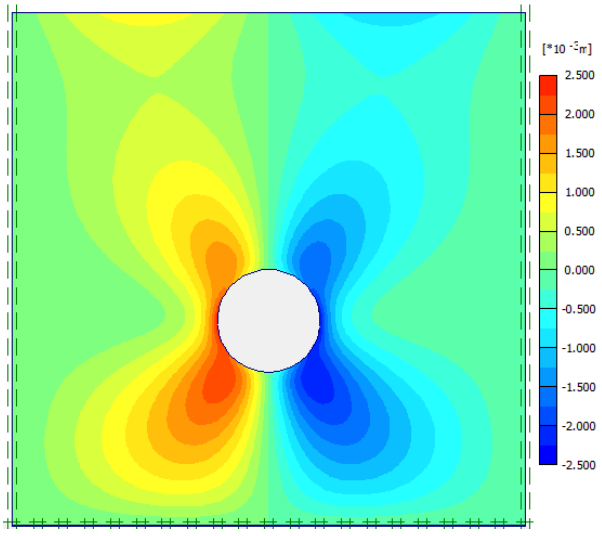


**Figure 5.5 (c)**

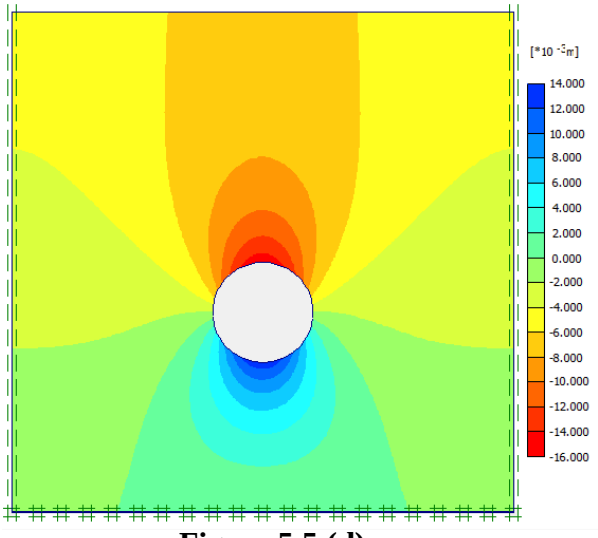


**Figure 5.5 (d)**

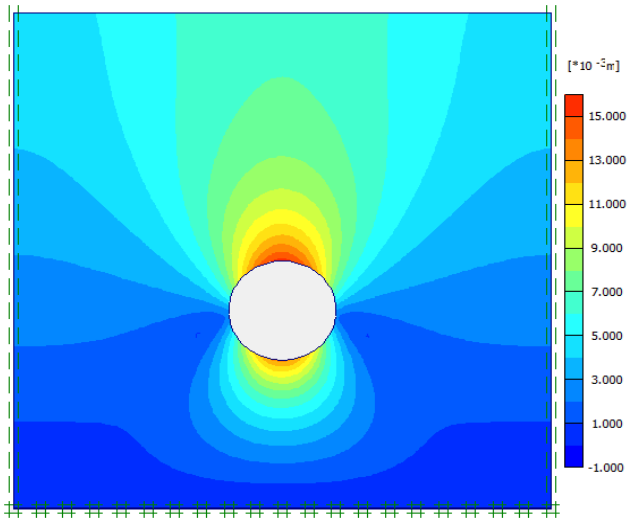


Figure 5.5 (e)

**Figure 5.5 : Tunnel of diameter 20m and insitu stress ratio 0.5 (a): Fine Mesh diagram (b): Stress Contours (c) Horizontal Displacements (d) Vertical Displacements (e) Total Displacements**

## CIRCULAR TUNNEL OF DIAMETER 25m

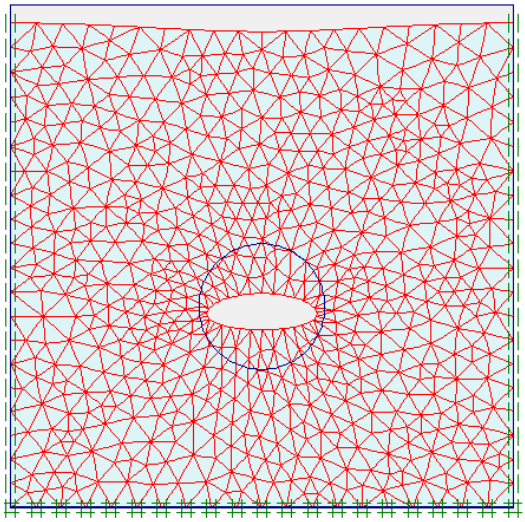

**Figure 5.6 (a)**

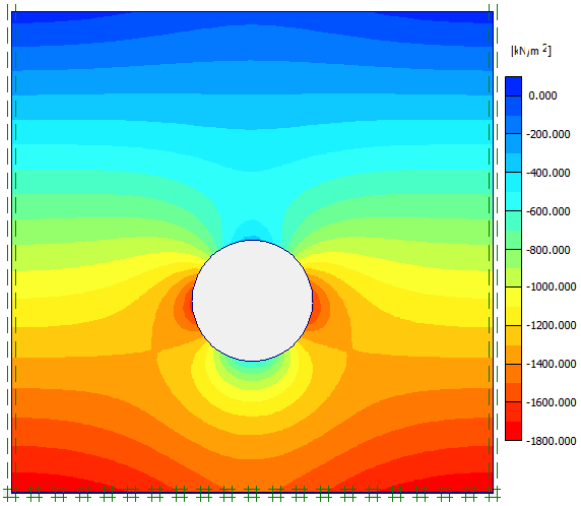


**Figure 5.6 (b)**

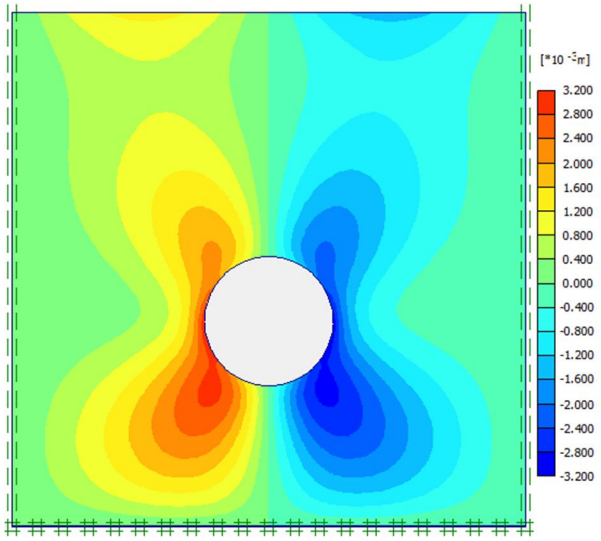


**Figure 5.6 (c)**

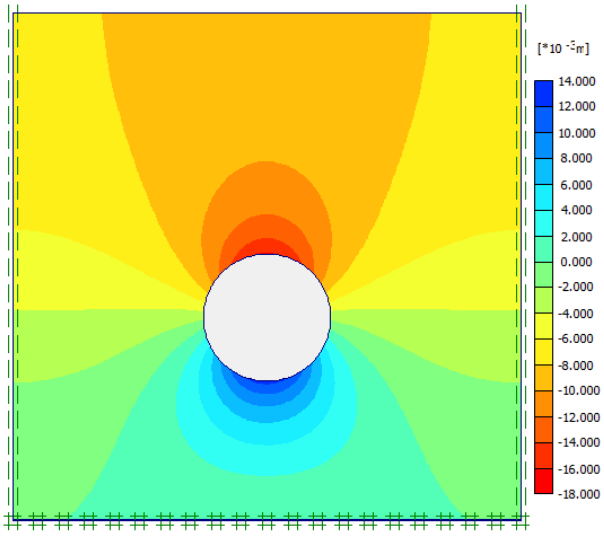


**Figure 5.6 (d)**

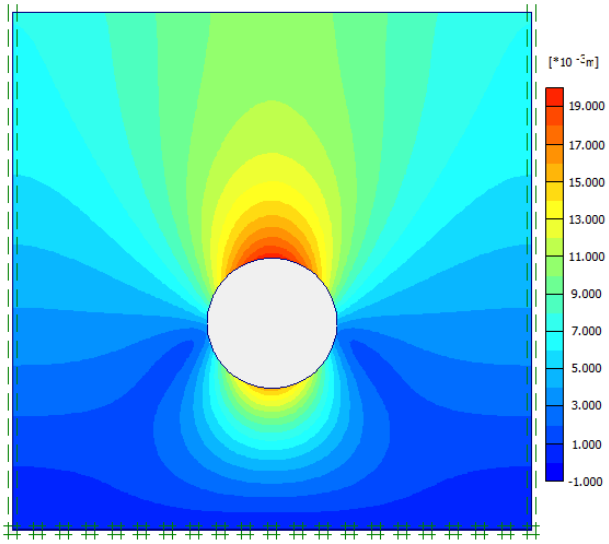


Figure 5.6 (e)

**Figure 5.6 : Tunnel of diameter 25m and insitu stress ratio 0.5 (a): Fine Mesh diagram (b): Stress Contours (c) Horizontal Displacements (d) Vertical Displacements (e) Total Displacements**

## CIRCULAR TUNNEL OF DIAMETER 30m

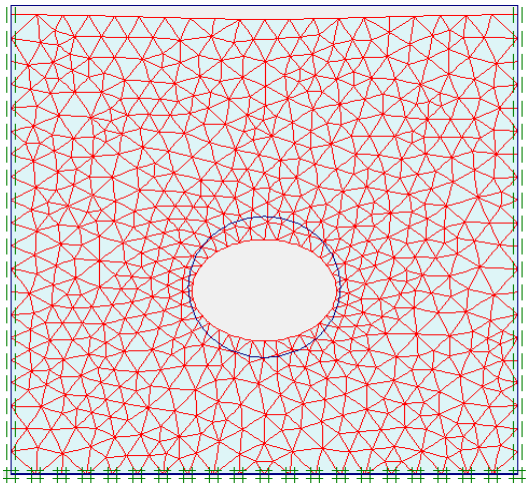

Figure 5.7 (a)

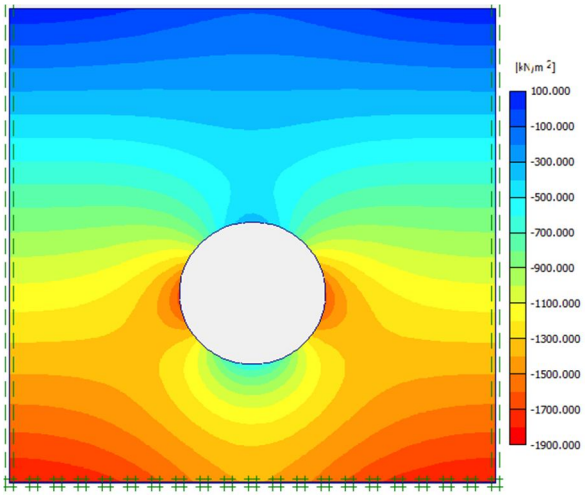


Figure 5.7 (b)

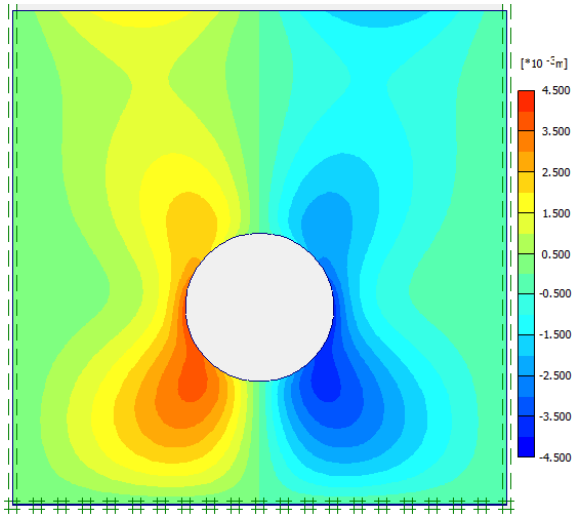


Figure 5.7 (c)

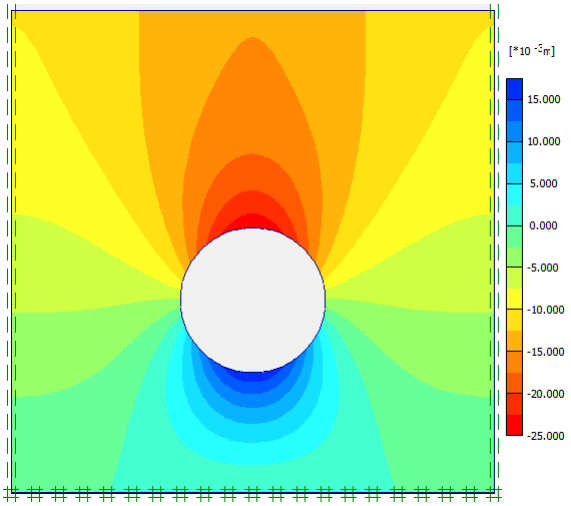


Figure 5.7 (d)

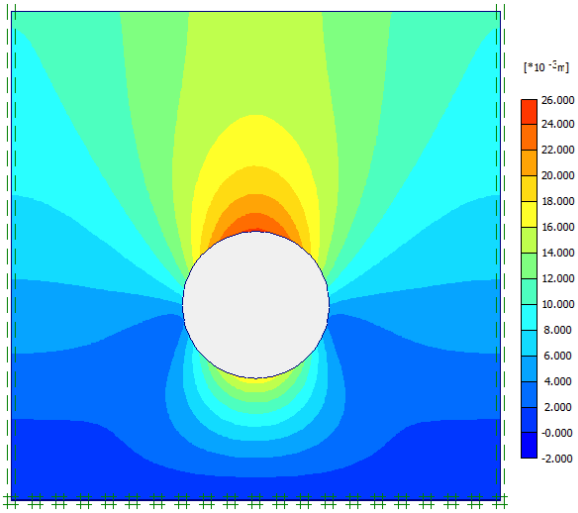


Figure 5.7 (e)

**Figure 5.7 : Tunnel of diameter 30m and insitu stress ratio 0.5 (a): Fine Mesh diagram (b): Stress Contours (c) Horizontal Displacements (d) Vertical Displacements (e) Total Displacements**

## INSITU STRESS RATIO 1

## CIRCULAR TUNNEL OF DIAMETER 5m

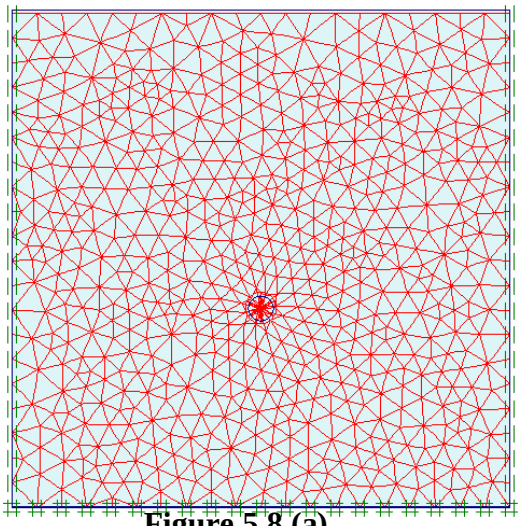

Figure 5.8 (a)

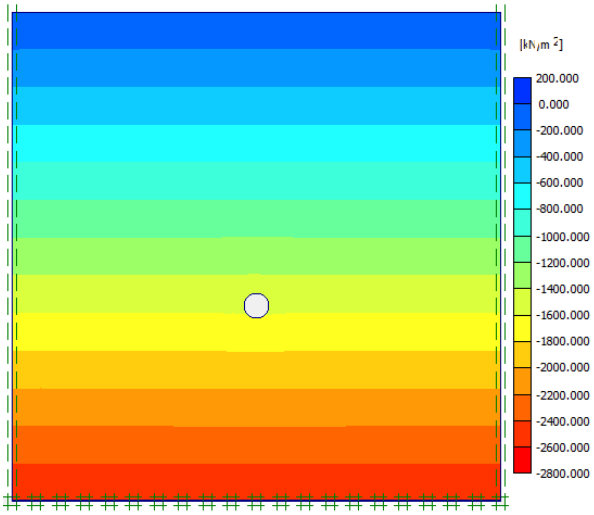


Figure 5.8 (b)

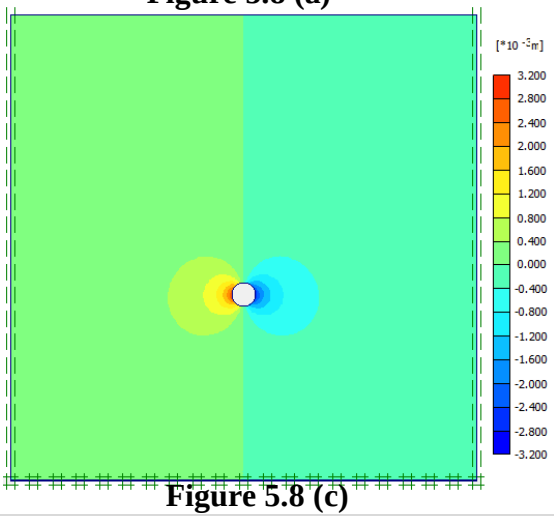


Figure 5.8 (c)

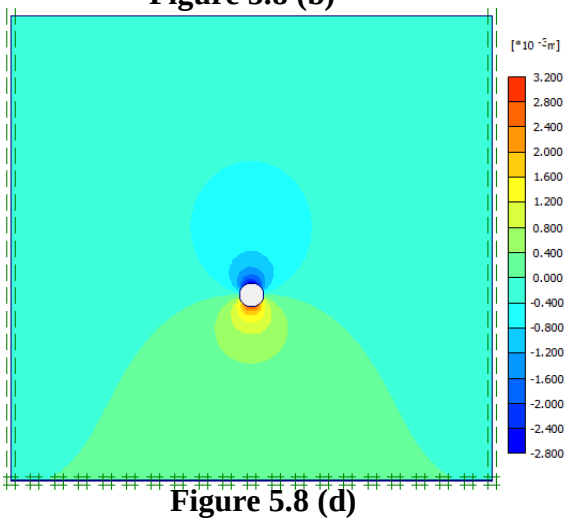


Figure 5.8 (d)

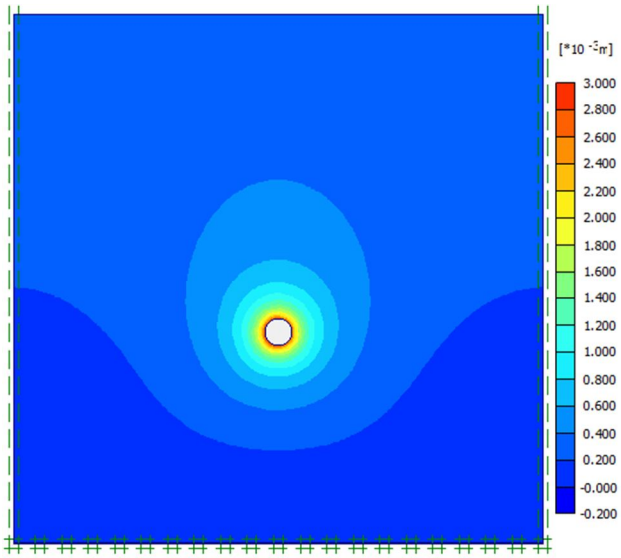


**Figure 5.8 (e)**

**Figure 5.8 : Tunnel of diameter 5m and insitu stress ratio 1 (a): Fine Mesh diagram (b): Stress Contours (c) Horizontal Displacements (d) Vertical Displacements (e) Total Displacements**

## CIRCULAR TUNNEL OF DIAMETER 10m

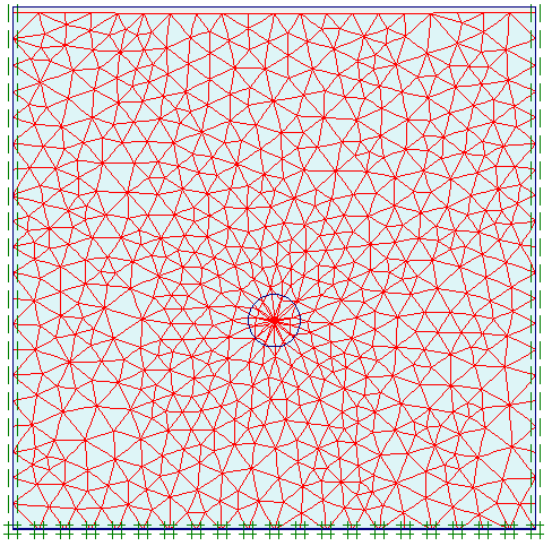

**Figure 5.9 (a)**

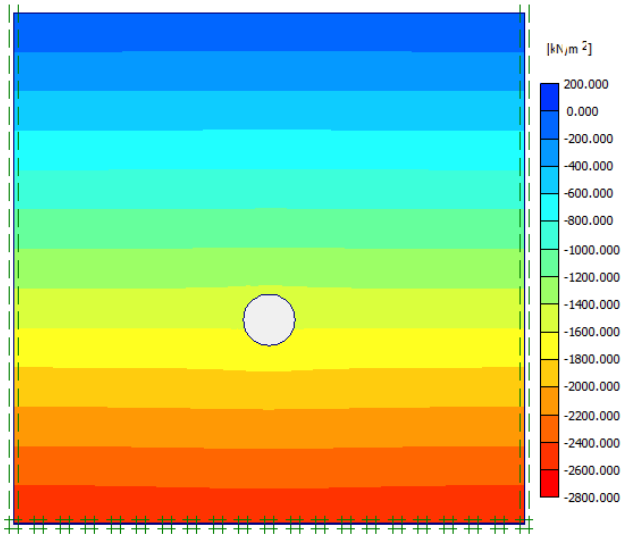


**Figure 5.9 (b)**

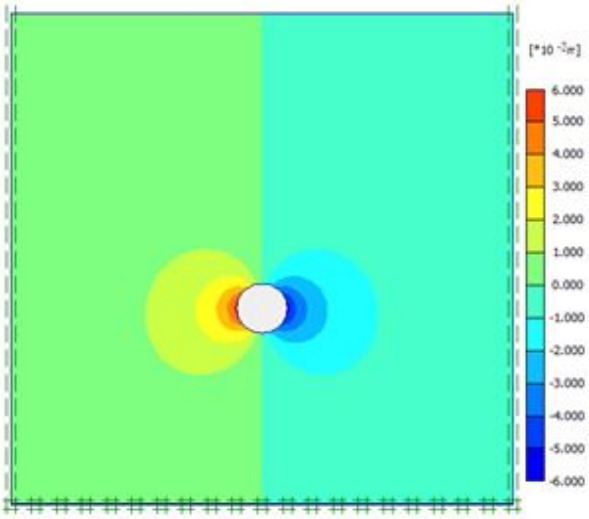


**Figure 5.9 (c)**

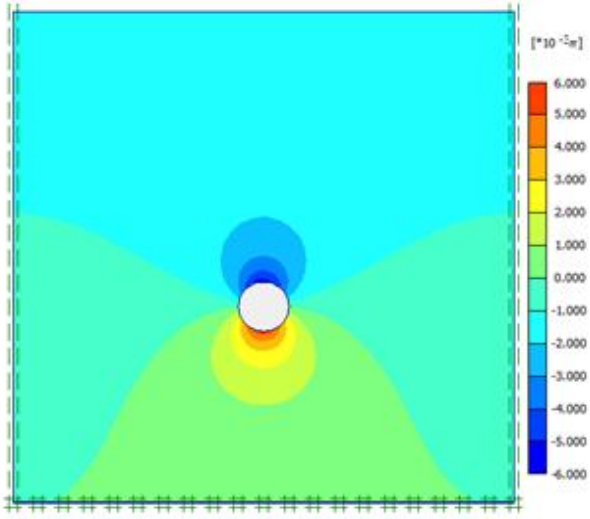


**Figure 5.9 (d)**

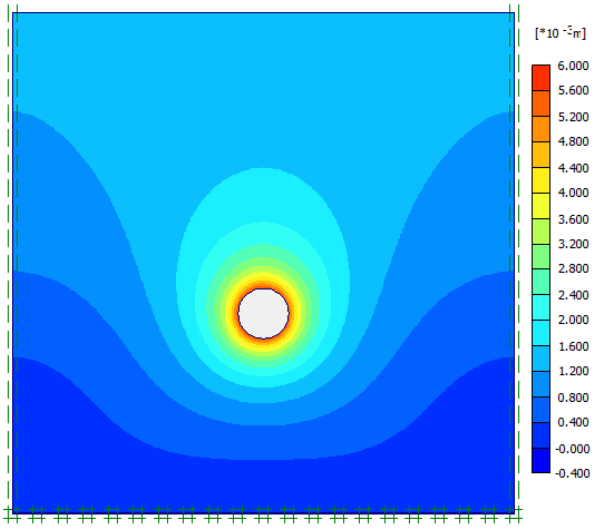


Figure 5.9 (e)

**Figure 5.9 : Tunnel of diameter 10m and insitu stress ratio 1 (a): Fine Mesh diagram (b): Stress Contours (c) Horizontal Displacements (d) Vertical Displacements (e) Total Displacements**

## CIRCULAR TUNNEL OF DIAMETER 15m

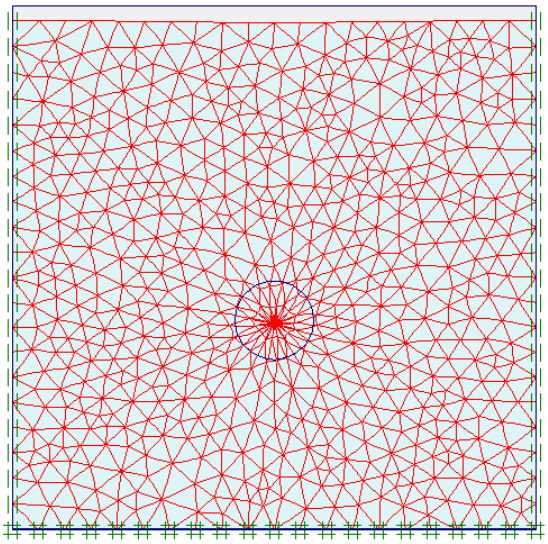

Figure 5.10 (a)

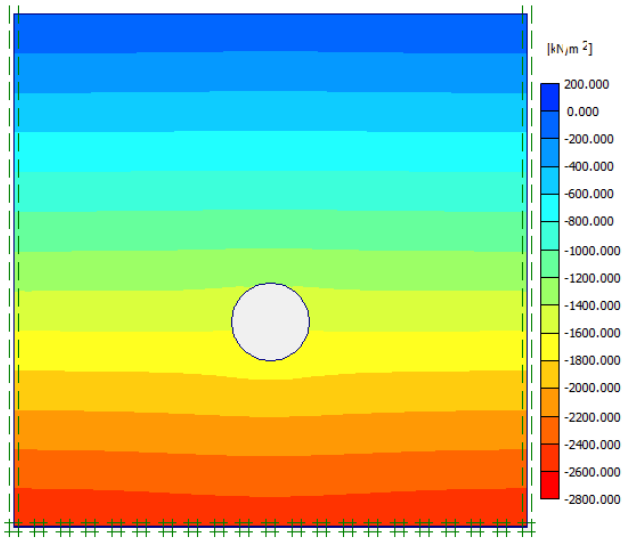


Figure 5.10 (b)

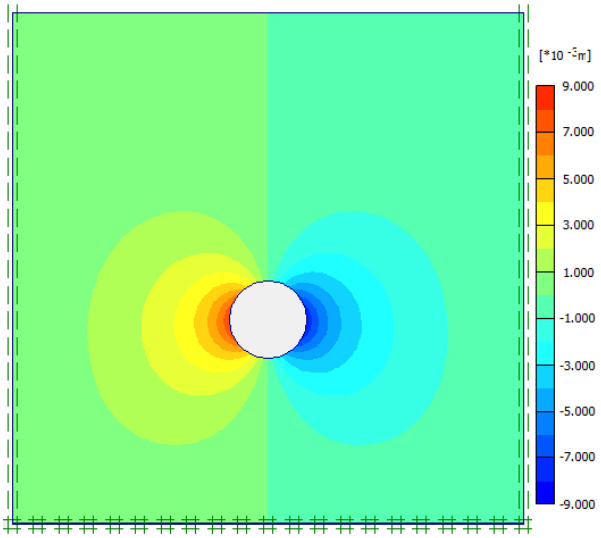


Figure 5.10 (c)

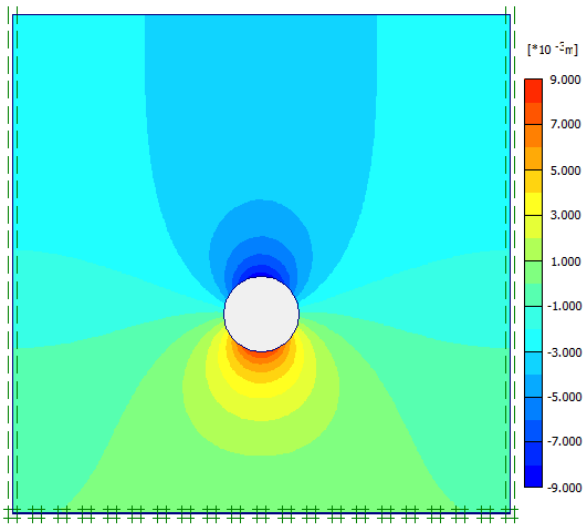


Figure 5.10 (d)

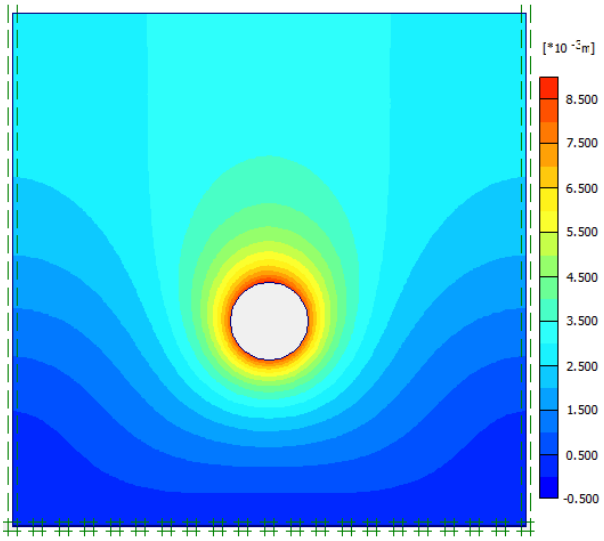


**Figure 5.10 (e)**

**Figure 5.10 : Tunnel of diameter 15m and insitu stress ratio 1 (a): Fine Mesh diagram (b): Stress Contours (c) Horizontal Displacements (d) Vertical Displacements (e) Total Displacements**

## CIRCULAR TUNNEL OF DIAMETER 20m

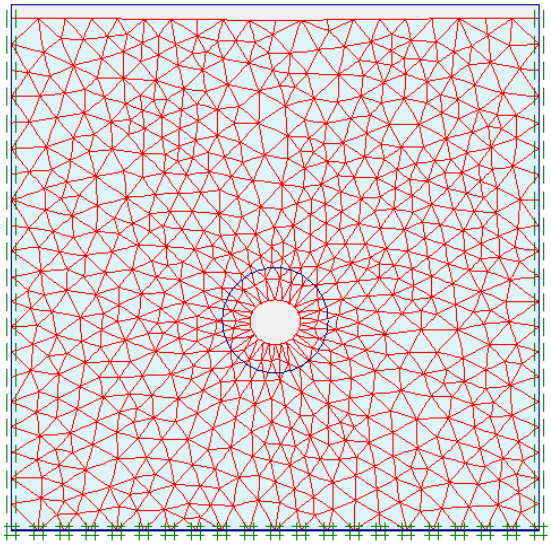

**Figure 5.11 (a)**

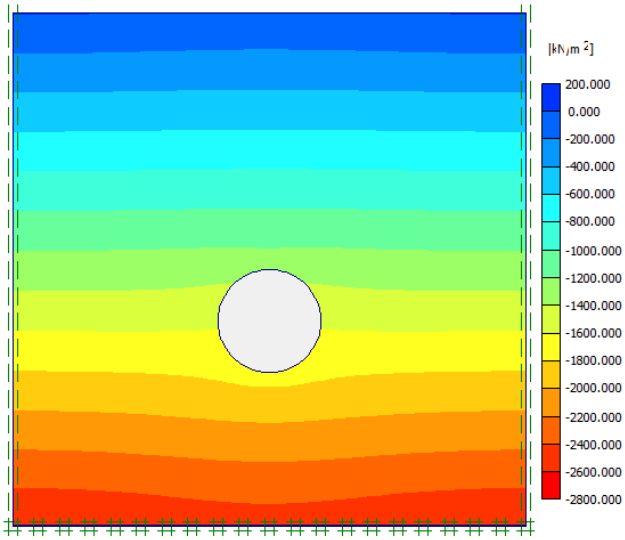


**Figure 5.11 (b)**

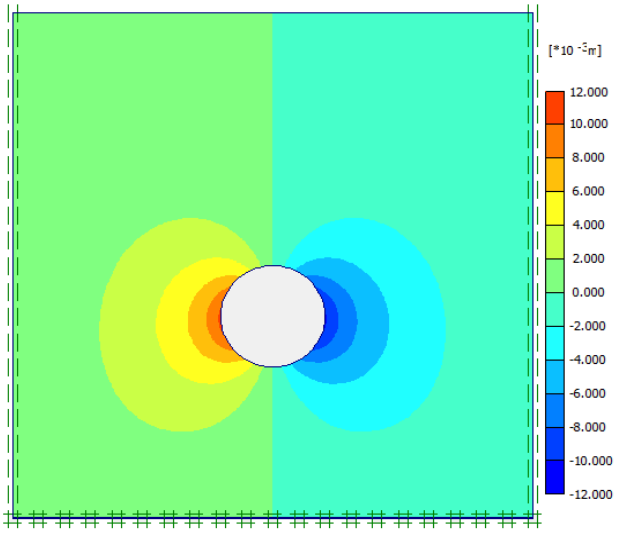


**Figure 5.11 (c)**

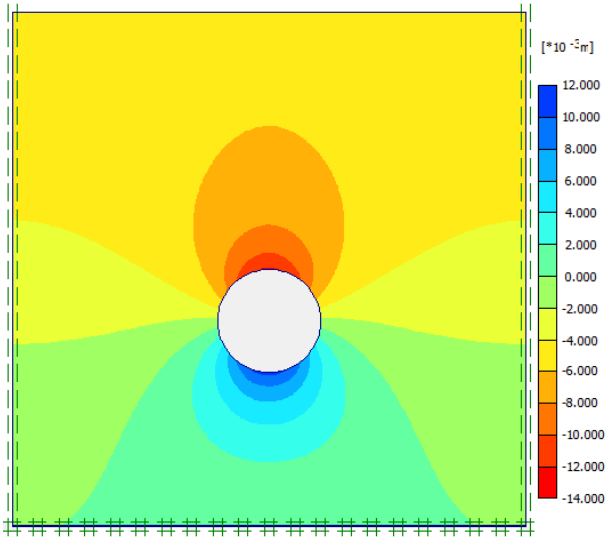


**Figure 5.11 (d)**

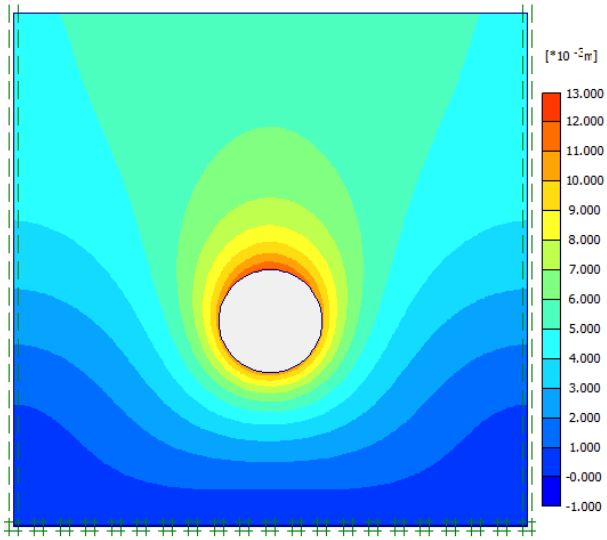


Figure 5.11 (e)

**Figure 5.11 : Tunnel of diameter 20m and insitu stress ratio 1 (a): Fine Mesh diagram (b): Stress Contours (c) Horizontal Displacements (d) Vertical Displacements (e) Total Displacements**

## CIRCULAR TUNNEL OF DIAMETER 25m

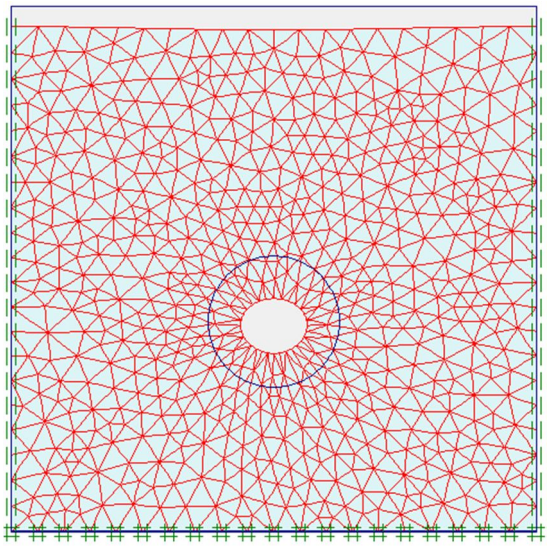

Figure 5.12 (a)

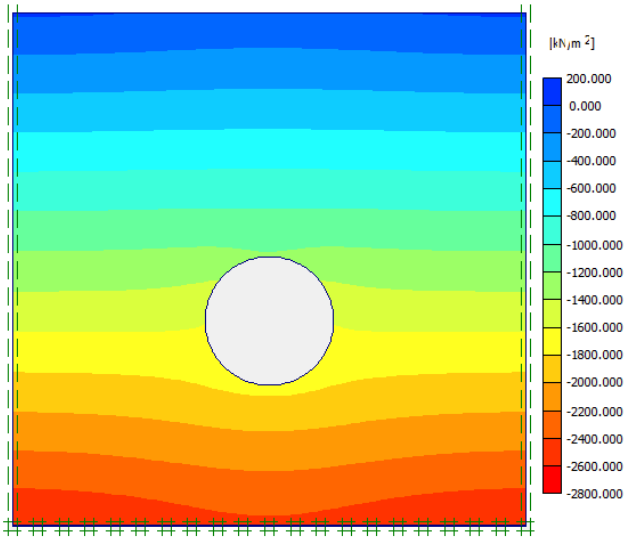


Figure 5.12 (b)

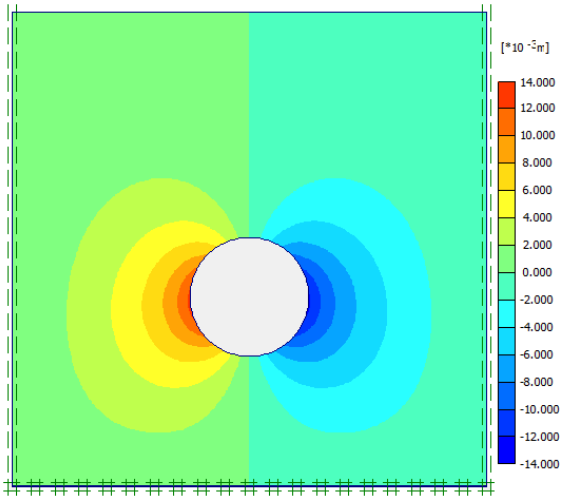


Figure 5.12 (c)

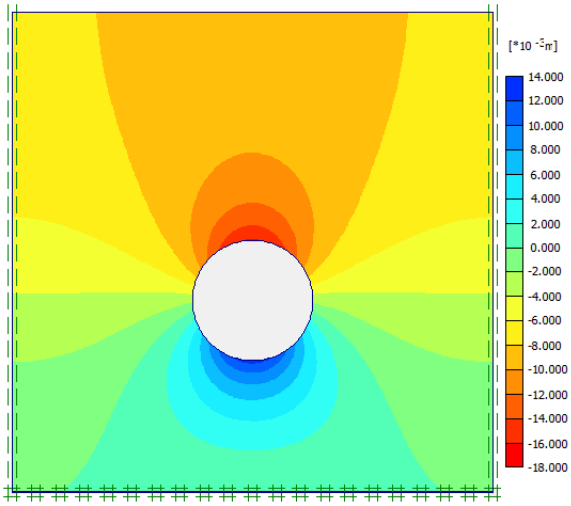


Figure 5.12 (d)

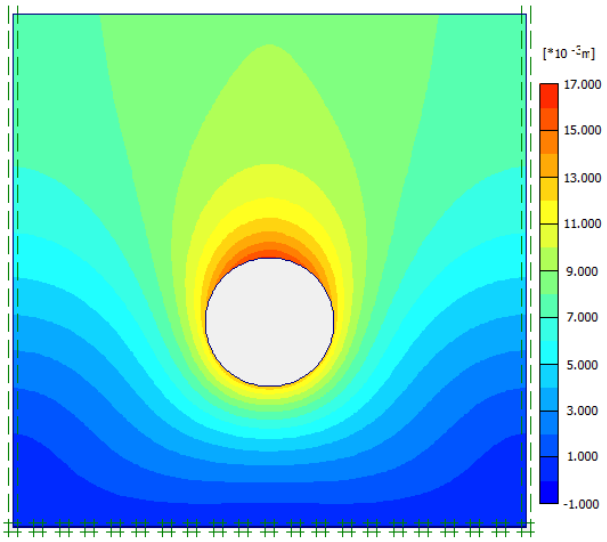


**Figure 5.12 (e)**

**Figure 5.12 : Tunnel of diameter 25m and insitu stress ratio 1 (a): Fine Mesh diagram (b): Stress Contours (c) Horizontal Displacements (d) Vertical Displacements (e) Total Displacements**

## CIRCULAR TUNNEL OF DIAMETER 30m

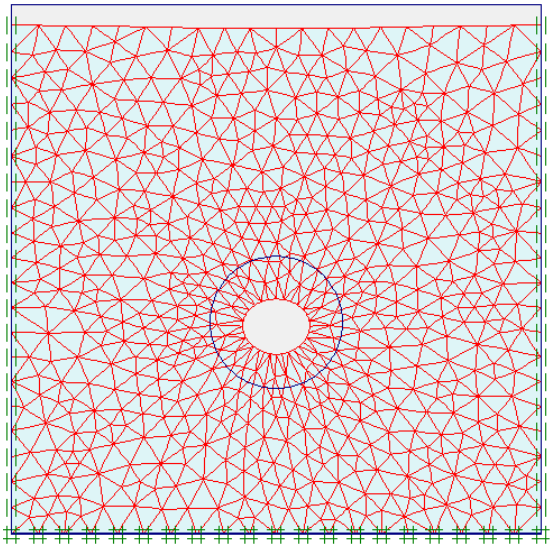

**Figure 5.13 (a)**

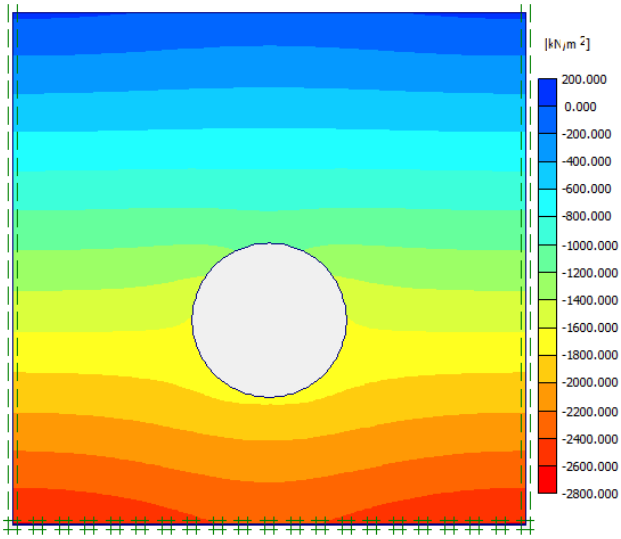


**Figure 5.13 (b)**

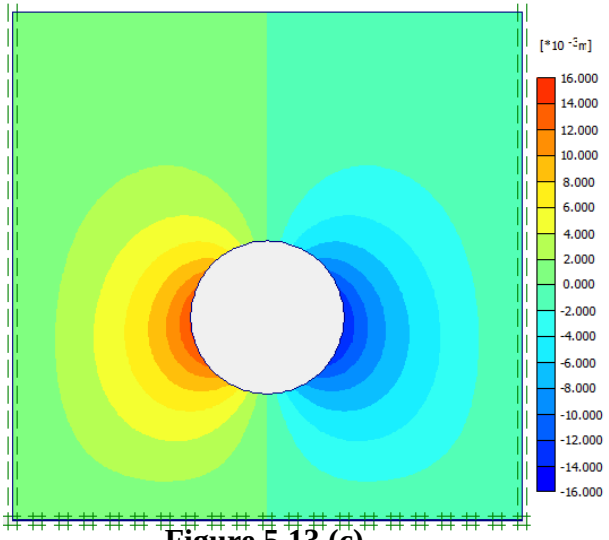


**Figure 5.13 (c)**

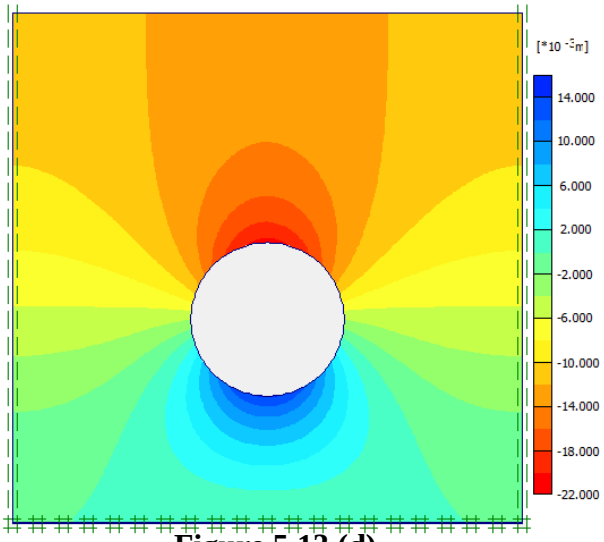


**Figure 5.13 (d)**

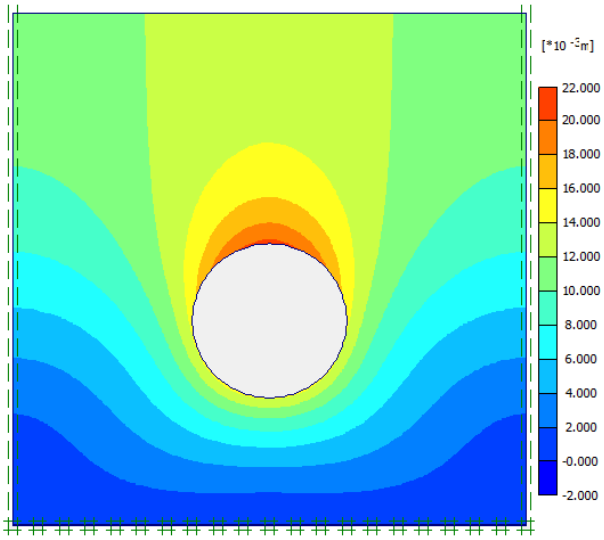


Figure 5.13 (e)

**Figure 5.13 : Tunnel of diameter 30m and insitu stress ratio 1 (a): Fine Mesh diagram (b): Stress Contours (c) Horizontal Displacements (d) Vertical Displacements (e) Total Displacements**

## INSITU STRESS RATIO 1.5

## CIRCULAR TUNNEL OF DIAMETER 5m

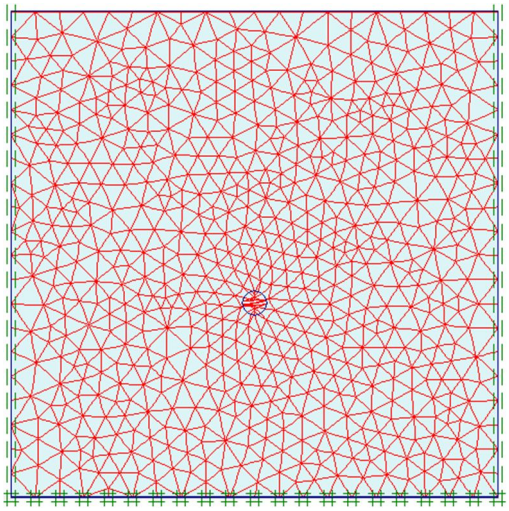

Figure 5.14 (a)

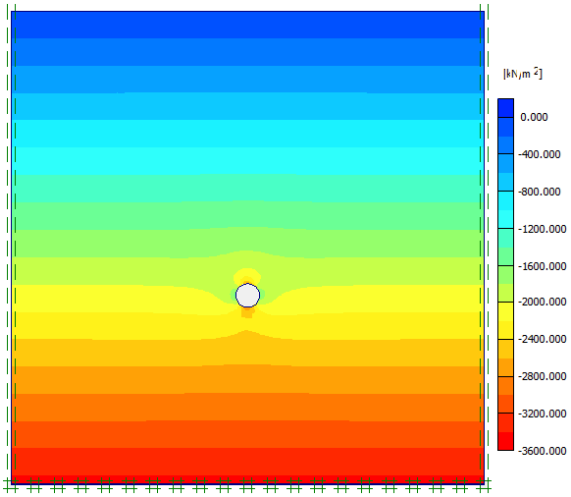


Figure 5.14 (b)

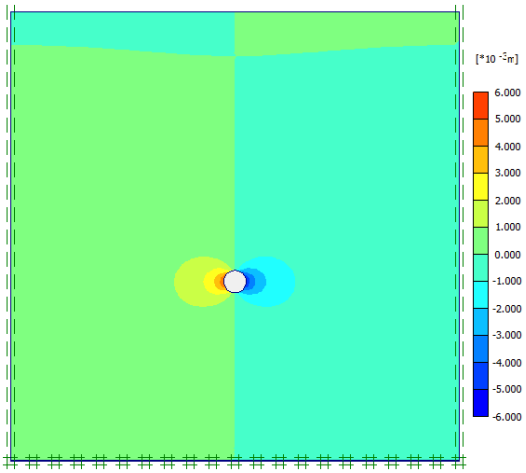


Figure 5.14 (c)

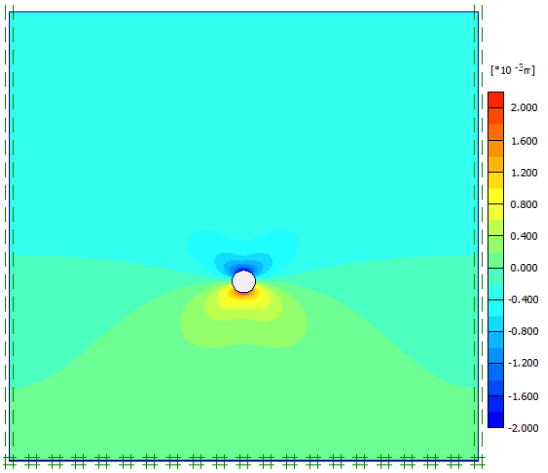


Figure 5.14 (d)

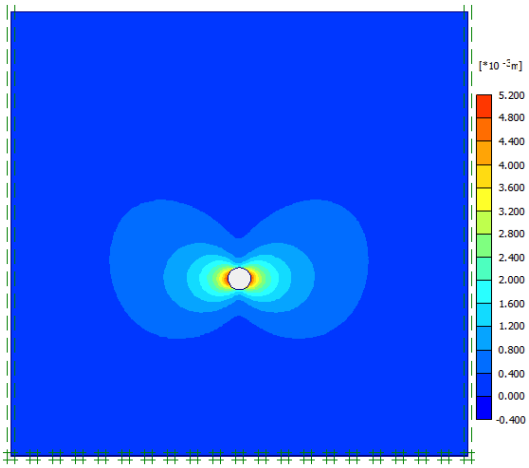


Figure 5.14 (e)

**Figure 5.14 : Tunnel of diameter 5m and insitu stress ratio 1.5 (a): Fine Mesh diagram (b): Stress Contours (c) Horizontal Displacements (d) Vertical Displacements (e) Total Displacements**

## CIRCULAR TUNNEL OF DIAMETER 10m

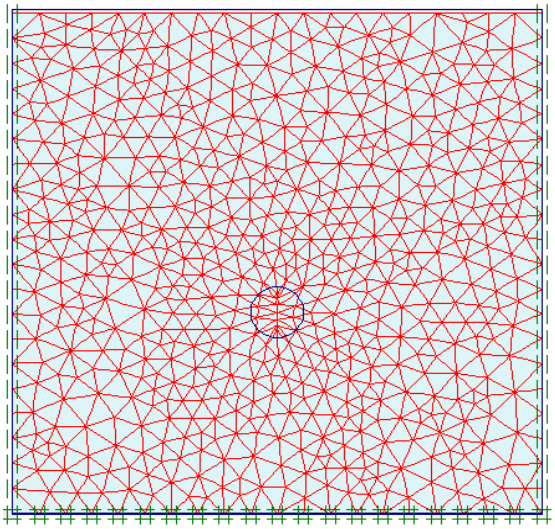

Figure 5.15 (a)

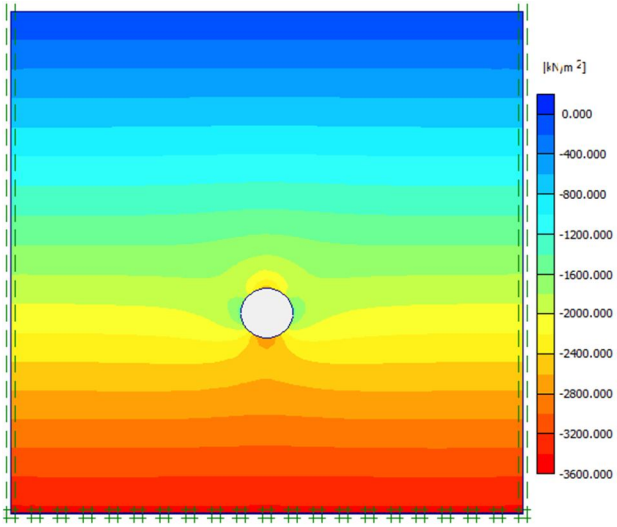


Figure 5.15 (b)

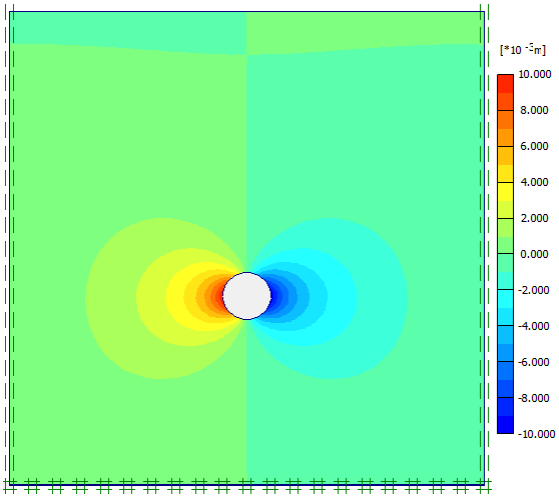


Figure 5.15 (c)

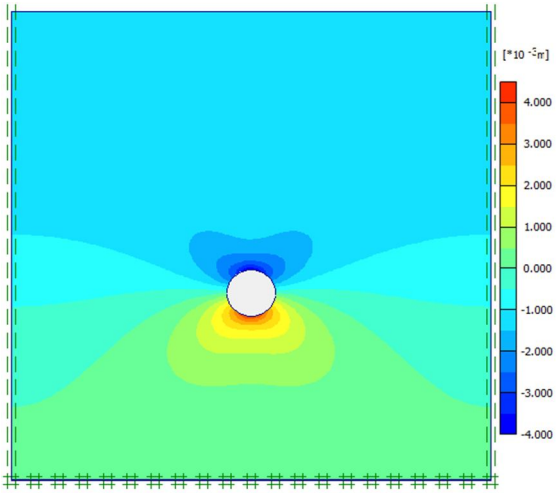


Figure 5.15 (d)

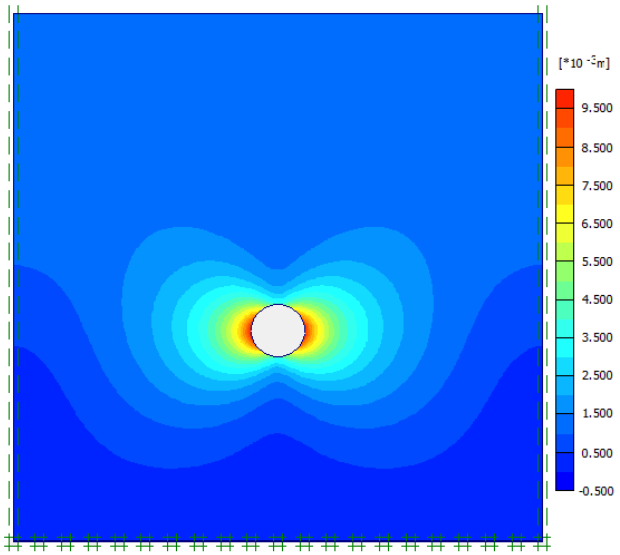


Figure 5.15 (e)

**Figure 5.15 : Tunnel of diameter 10m and insitu stress ratio 1.5 (a): Fine Mesh diagram (b): Stress Contours (c) Horizontal Displacements (d) Vertical Displacements (e) Total Displacements**

## CIRCULAR TUNNEL OF DIAMETER 15m

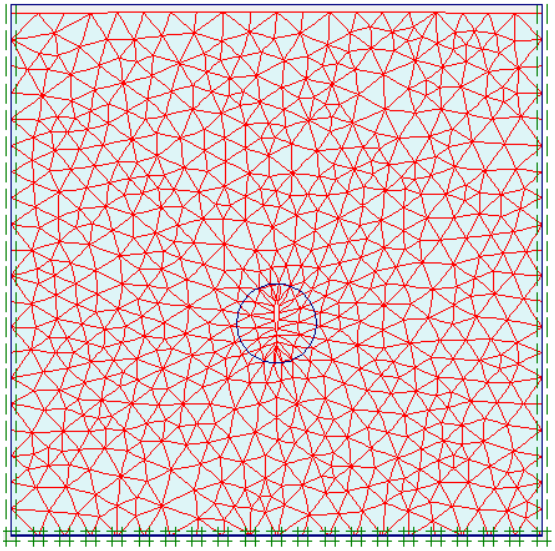

Figure 5.16 (a)

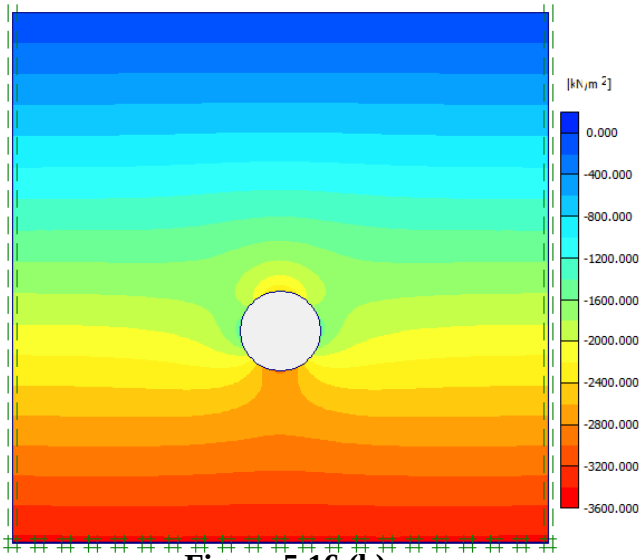


Figure 5.16 (b)

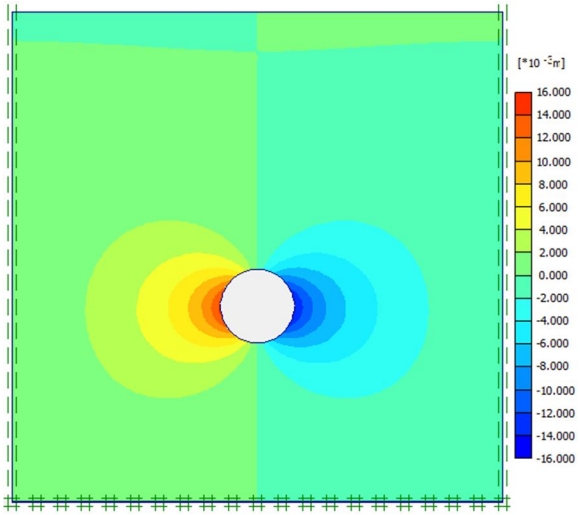


Figure 5.16 (c)

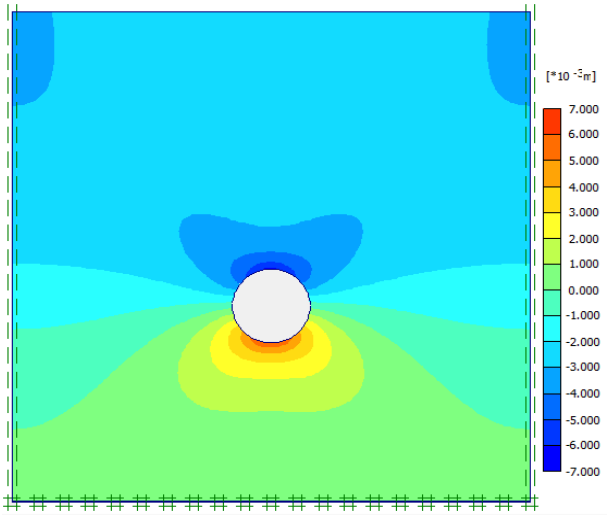


Figure 5.16 (d)

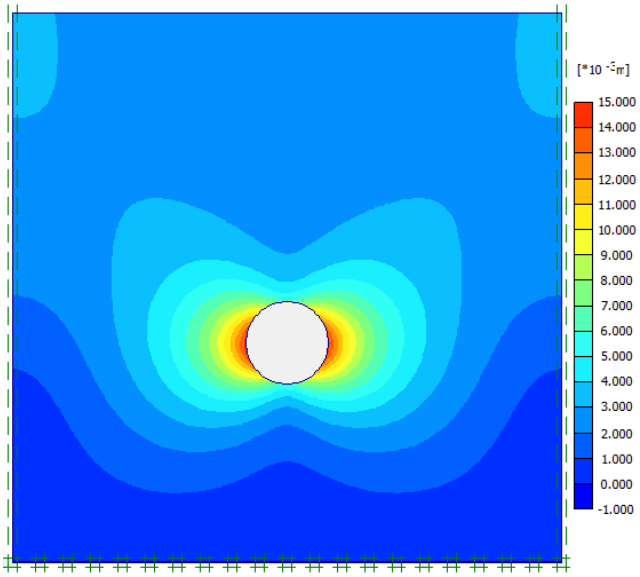


Figure 5.16 (e)

**Figure 5.16 : Tunnel of diameter 15m and insitu stress ratio 1.5 (a): Fine Mesh diagram (b): Stress Contours (c) Horizontal Displacements (d) Vertical Displacements (e) Total Displacements**

## CIRCULAR TUNNEL OF DIAMETER 20m

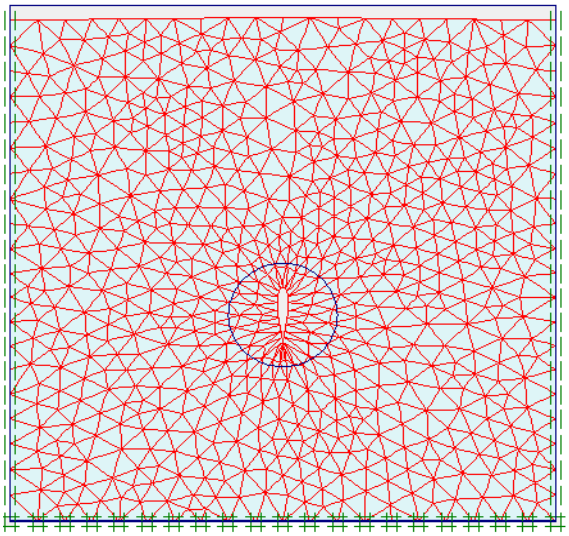

Figure 5.17 (a)

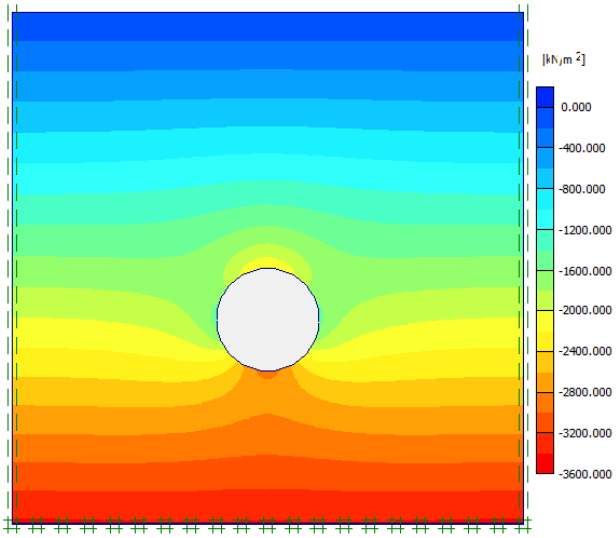


Figure 5.17 (b)

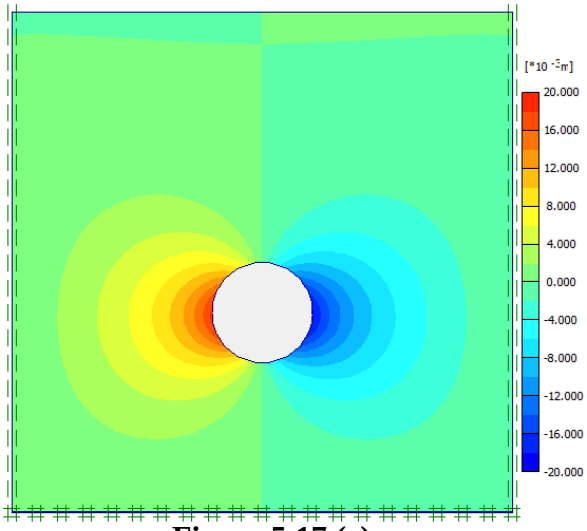


Figure 5.17 (c)

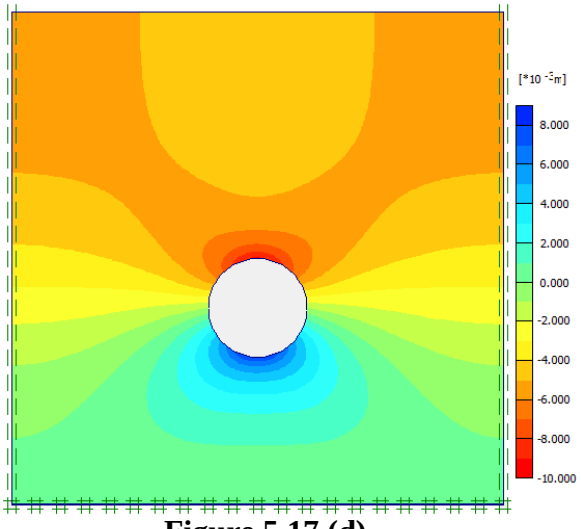


Figure 5.17 (d)

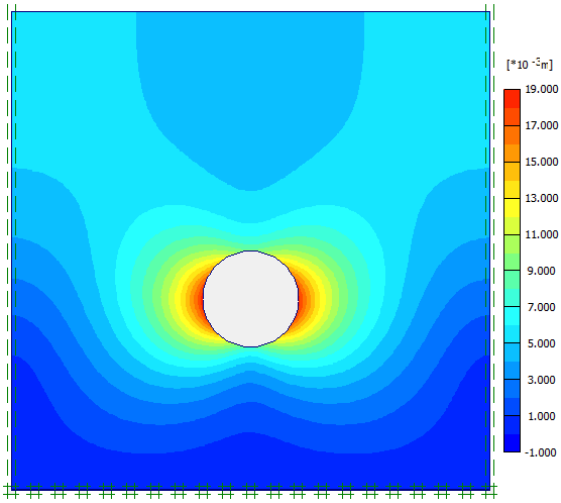


Figure 5.17 (e)

**Figure 5.17 : Tunnel of diameter 20m and insitu stress ratio 1.5 (a): Fine Mesh diagram (b): Stress Contours (c) Horizontal Displacements (d) Vertical Displacements (e) Total Displacements**

## CIRCULAR TUNNEL OF DIAMETER 25m

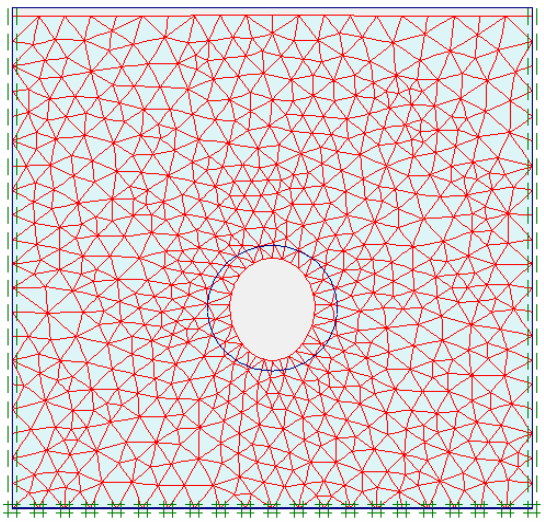

Figure 5.18 (a)

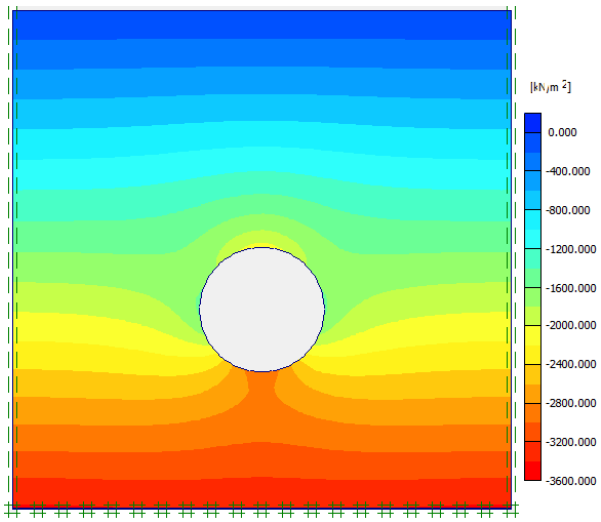


Figure 5.18 (b)

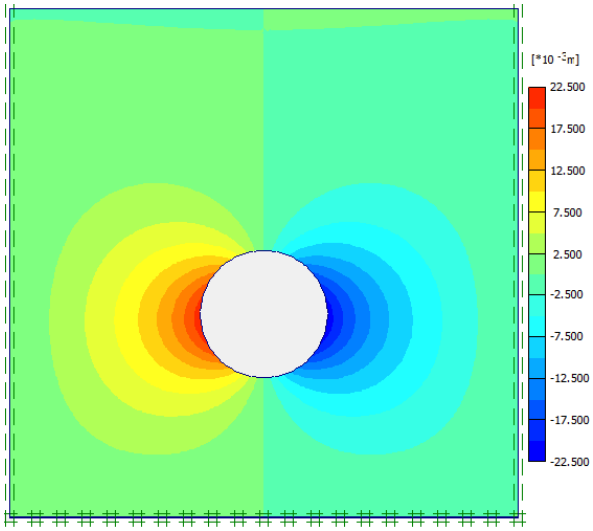


Figure 5.18 (c)

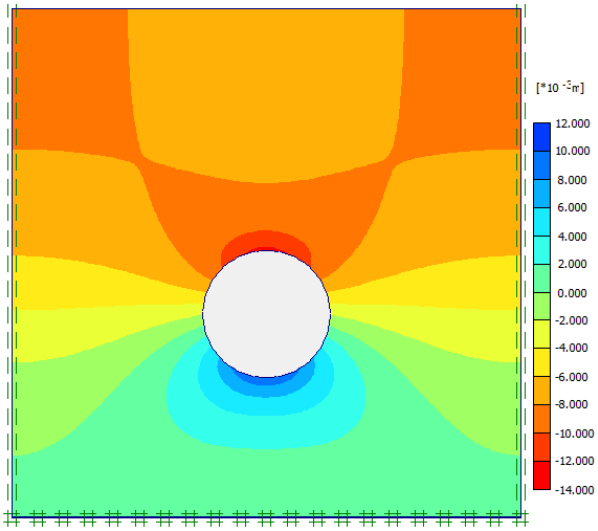


Figure 5.18 (d)

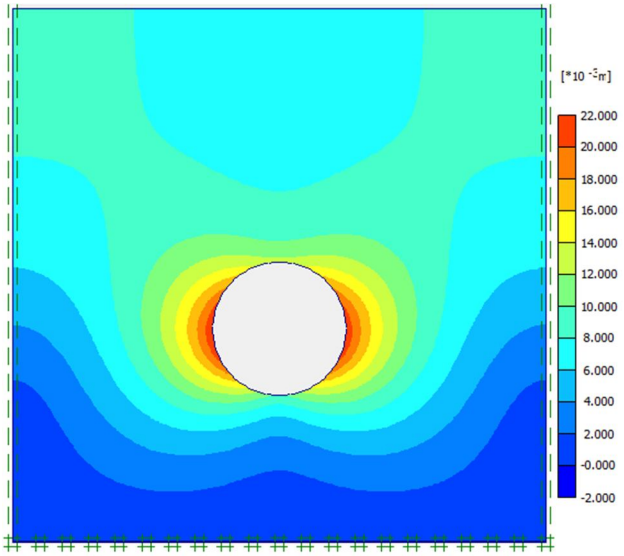


**Figure 5.18 (e)**

**Figure 5.18 : Tunnel of diameter 25m and insitu stress ratio 1.5 (a): Fine Mesh diagram (b): Stress Contours (c) Horizontal Displacements (d) Vertical Displacements (e) Total Displacements**

## CIRCULAR TUNNEL OF DIAMETER 30m

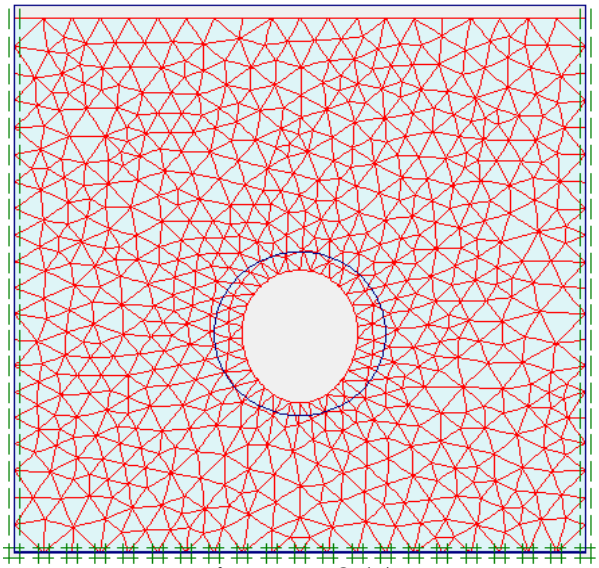

**Figure 5.19 (a)**

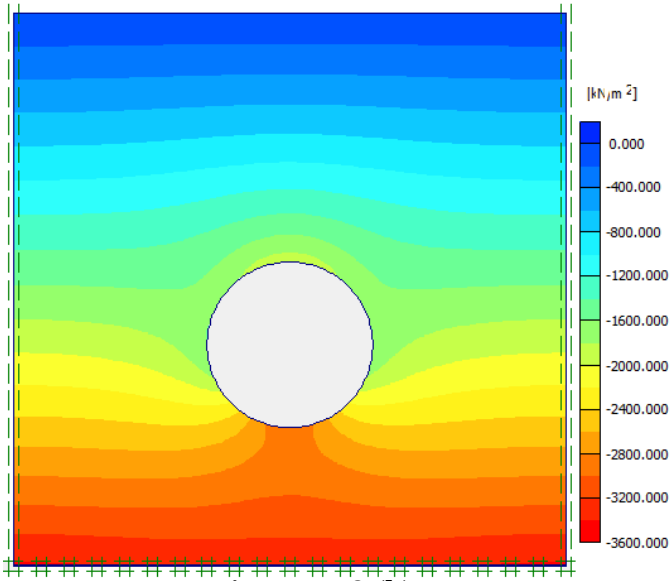


**Figure 5.19 (b)**

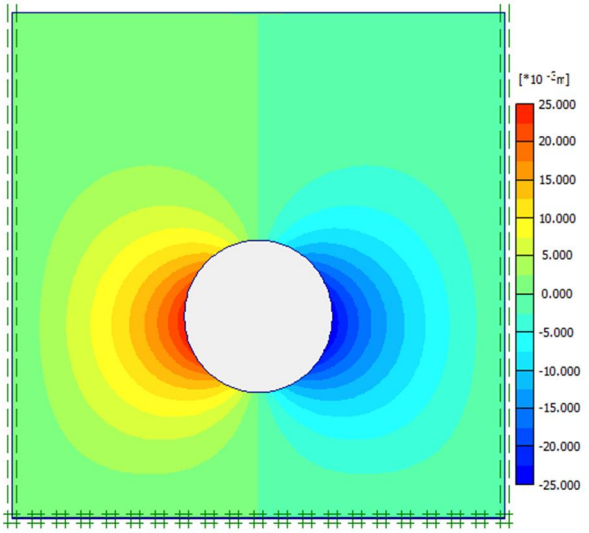


**Figure 5.19 (c)**

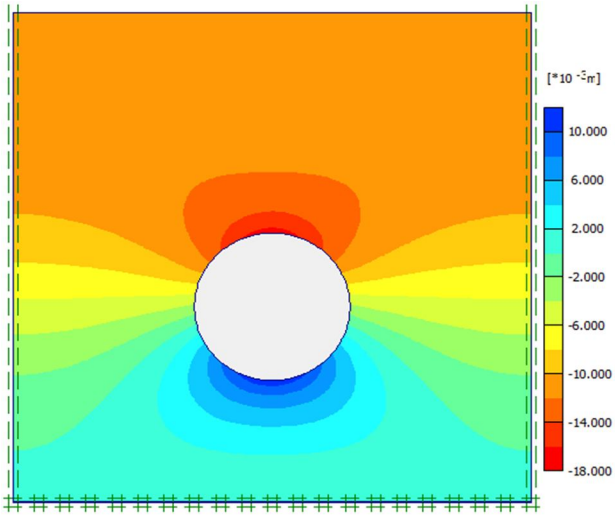


**Figure 5.19 (d)**

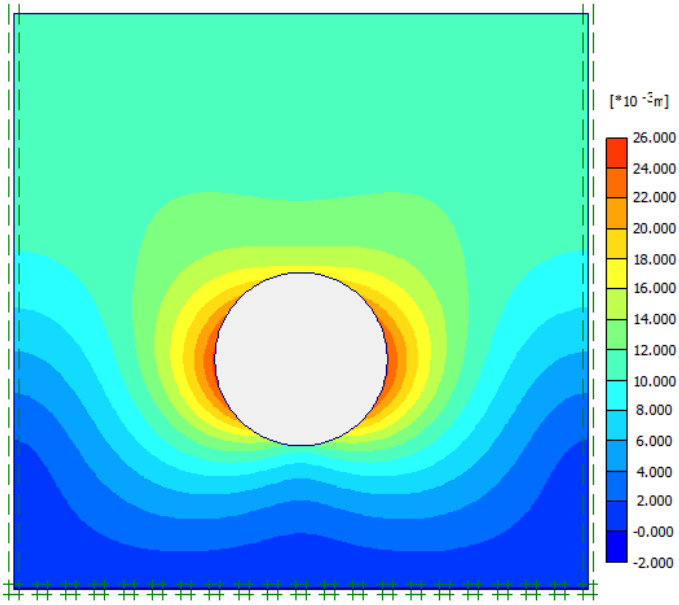


**Figure 5.19 (e)**

**Figure 5.19 : Tunnel of diameter 30m and insitu stress ratio 1.5 (a): Fine Mesh diagram (b): Stress Contours (c) Horizontal Displacements (d) Vertical Displacements (e) Total Displacements**

The deformations and stresses in the rock tunnel system are determined for tunnels of different diameters and insitu ratios which are shown above in the form of contours. From the results obtained, various inferences can be made. All the results obtained are same on the both sides of the vertical axis of the tunnel which is passing through the centre, this is due to the symmetry of the model.

The maximum horizontal displacement occurs at the centre of the sidewall (also called spring line) which is in the opposite directions for both the spring lines as can be inferred from the figures. The horizontal displacement decreases from the tunnel surface as the distance from the surface is increased. The maximum vertical deformation occurs at the centre of the top surface of the tunnel (also called crown). Due to the overburden pressure, the settlement at the crown occurs in the downward direction. Also, the settlement increases gradually from the ground surface up to the crown of the tunnel. The vertical displacement at the bottom surface of the tunnel (also called invert) occurs is in the upward direction. At points below the invert, the vertical displacement gradually decreases with the distance from the invert.

The settlement at the crown and the upward displacement at the invert cause change in the stresses at the crown and the invert which are tensile in nature in the vertical direction. The horizontal displacement at both of the spring lines in the opposite direction cause change in the stresses at the spring line which are compressive in nature.

The maximum horizontal displacement which occurs at the spring line of the tunnel increases with the increase in the diameter of the tunnel whose variation under different insitu stress ratios is shown with the help of the graph in the Figure 5.20 . The maximum settlement which occurs at the crown of the tunnel increases with the increase in the diameter of the tunnel whose variation under different values of insitu stress ratios whose variation is shown with the help of the graph in the Figure 5.21 .

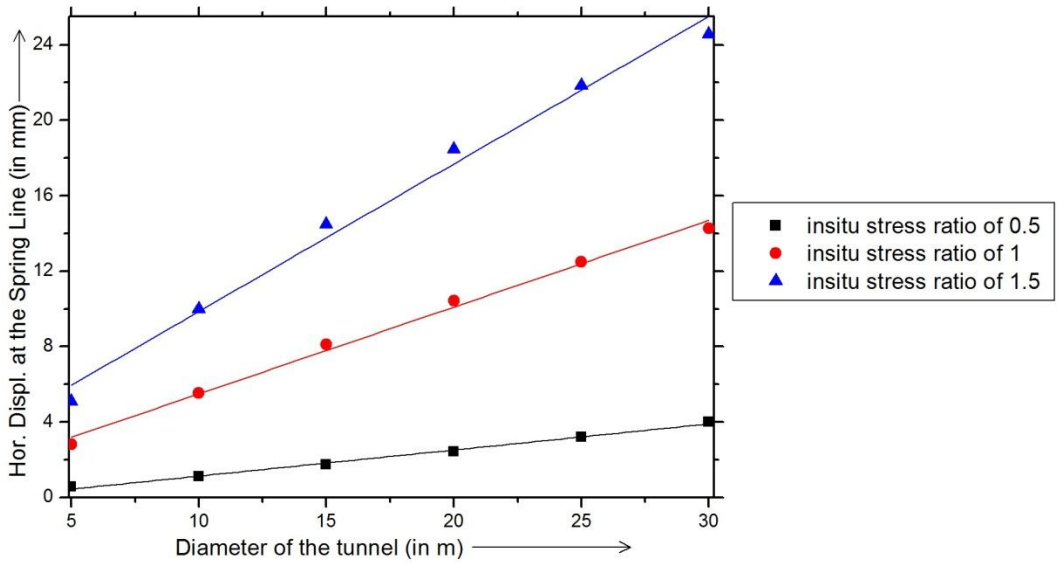


**Figure 5.20 : Variation of Horizontal Displacement at the Spring Line of the Tunnel with different diameters and insitu stress ratios**

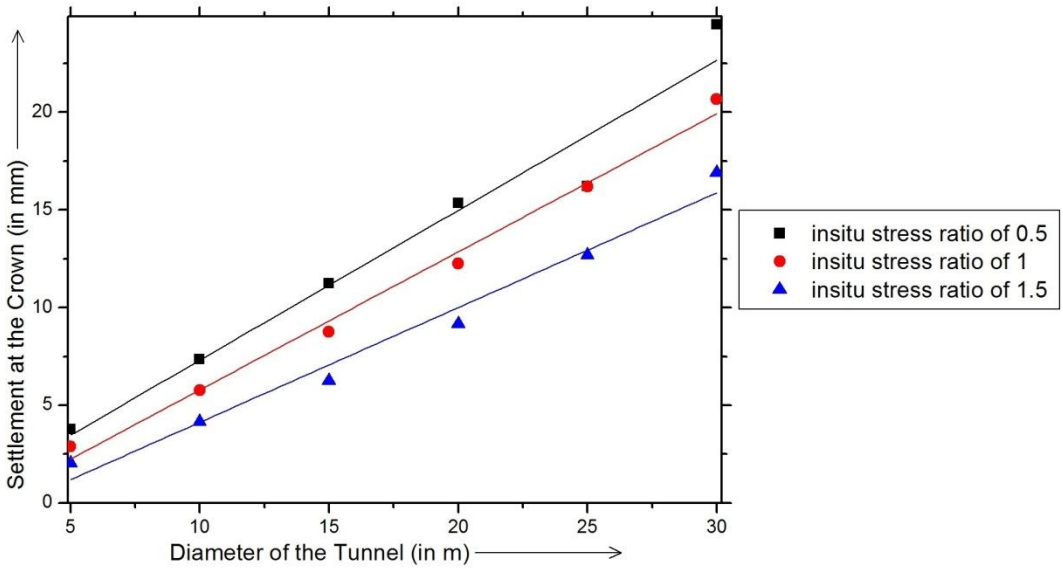


**Figure 5.21 : Variation of Settlement at the Crown of the Tunnel with different diameters and insitu stress ratios**

# CHAPTER 6

# CONCLUSIONS

# AND

# FUTURE SCOPE

## CONCLUSIONS

- Based on the properties of the schist rock as obtained from the experimental results, the rock is suitable for the following applications:
    - Construction of breakwater systems and other earthworks against erosion by water in the form of riprap.
    - Putting as ballast to support railwaysleepers.
    - As a base, sub-base , top course of roads.
    - Making monuments and sculptures.
- The Elastic Modulus and Uniaxial Compressive Strength values of the jointed rock sample decreases on increasing the Joint Orientation upto an angle of about $40^{o}$ and thereafter starts increasing.
- The following correlations are proposed for prediction of strength in Schist rock in presence of joints

  $\sigma_{cr} = exp(-0.6308 J_f)$ and $E_{tr} = exp(-0.1242 J_f)$
- The results for Elastic Modulus ratio obtained from the present experimental study are consistent to some extent with those of Arora(1987) and Padhy(2005) whereas those of Compressive Strength ratio are not so consistent.
- The horizontal displacement at the Spring Line of the the tunnel increases linearly with the increase in diameter of the tunnel. Also, when a particular diameter of tunnel is considered the horizontal displacement at the Spring Line increases with the increase in the insitu stress ratio.
- The vertical settlement at the Crown of the the tunnel increases linearly with the increase in diameter of the tunnel. Also, when a particular diameter of tunnel is considered the vertical settlement at the Crown decreases with the increase in the insitu stress ratio.

## FUTURE SCOPES

- Using the properties of the rock as obtained from the experimental results of the present study, different engineering rock structures can be modelled and analyzed.
- The behaviour of the jointed rocks can also be studied and analyzed by using a filler material such as Cement and others.

# CHAPTER 7

# REFERENCES

# REFERENCES


- A. A. Elsayed (2011), '*Study of rock-lining interaction for circular tunnels using finite element analysis'*, Jordan Journal of Engineering, Vol 5, No.1
- E. Hoek and E. T. Brown (1997), '*Practical estimates of rock mass strength'*, International Journal of Rock Mechanics and Mining Sciences, Vol 34, No 8, pp1165-1186
- K. Sheshadri Rao, T. Ramamurthy and G. Venkappa Rao (1984), '*Strength and deformation behaviour of Sandstones'*, PhD Thesis, IIT Delhi
- Raghavendra V. , Stanley Jose, G. H. Arjun Shounak and T. G. Sitaram (2015), '*Finite element analysis of underground metro tunnels'*, International Journal of Civil Engineering and Technology, Vol 6, Issue 2, pp 6-15
- Rajendra P. Tiwari and K. Seshagiri Rao (2006), '*Post failure behaviour of a rock mass under the influence of triaxial and true triaxial confinement'*, Engineering Geology 84, pp 112-129
- R. K. Srivastava, A. Varadarajan and K. G. Sharma (1985), '*Elasto-plastic finite analyses of single and interacting tunnels'*, PhD Thesis, IIT Delhi
- R. K. Yaji, T. Ramamurthy and A. Varadarajan (1984), '*Shear strength and deformation response of jointed rocks'*, PhD Thesis, IIT Delhi
- T. Ramamurthy and V. K. Arora (1994), '*Strength Predictions for Jointed Rocks in Confined and Unconfined States'*, International Journal of Rock Mechanics, Mining Science and Geomechanics, Vol – 31, No. 1, pp 9-22
- ASTM C535-12, '*Standard test method for resistance to degradation of large-size coarse aggregate by abrasion and impact in the Los Angeles Machine'*
- ASTM D256-10, '*Standard test methods for determining the Izod Pendulum Impact Resistance'*
- IS 8764 – 2003, '*Method for determination of Point Load Strength Index of Rocks'*
- IS 9179 – 2001, '*Method for preparation of rock specimen for laboratory testing'*

- IS 9221 – 2001, '*Method for determination of Modulus of Elasticity and Poison's ratio of rock materials in Uniaxial Compression'*
- IS 10050 – 2001, '*Method for determination of Slake Durability Index of rocks'*
- IS 10082 – 2001, '*Method of test for determination of Tensile strength by indirect tests on rock specimen'*
- IS 12608 – 2005, '*Method for determination of Hardness of rock'*
- IS 13030 – 2001, '*Method of test for laboratory determination of Water Content, Porosity, Density and related properties of rock materia'l*
- IS 13047 – 2001, '*Method for determination of Strength of rock materials in triaxial compression'*